

Surprising diversity of non-classical silicon–hydrogen interactions in half-sandwich complexes of Nb and Ta: M–H ··· Si–Cl interligand hypervalent interaction (IHI) *versus* stretched and unstretched β–Si–H ··· M agostic bonding †

Georgii I. Nikonov,^{*a} Philip Mountford,^{*b} Stanislav K. Ignatov,^c Jennifer C. Green,^b Michael A. Leech,^e Lyudmila G. Kuzmina,^f Alexei G. Razuvaev,^c Nicholas H. Rees,^b Alexander J. Blake,^d Judith A. K. Howard^e and Dmitry A. Lemenovskii^a

^a Department of Chemistry, Moscow State University, Vorob'evy Gory, 119899 Moscow, Russia

^b Inorganic Chemistry Laboratory, South Parks Road, Oxford, UK OX1 3QR.

E-mail: philip.mountford@chem.ox.ac.uk

^c Department of Chemistry, Nizhny Novgorod State University, Gagarin Avenue 23, 603600 Nizhny Novgorod, Russia

^d School of Chemistry, University of Nottingham, University Park, Nottingham, UK NG7 2RD

^e Department of Chemistry, University of Durham, South Road, Durham, UK DH1 3LE

^f Institute of General and Inorganic Chemistry, RAS, Leninsky Prosp. 31, 117907 Moscow, Russia

Received 17th April 2001, Accepted 12th July 2001

First published as an Advance Article on the web 17th September 2001

Reaction of the niobium diphosphine compound [NbCp(NAr)(PMe₃)₂] (Ar = 2,6-C₆H₃Pr₂) with HSiMe₂Cl gives the formally d² silylamido derivative [NbCp{η³-N(Ar)SiMe₂-H}Cl(PMe₃)] **6**. X-Ray diffraction and NMR studies of this compound show that it has a stretched β-agostic Si–H → Nb interaction. Reaction of the related precursor [NbCp(NAr')(PMe₃)₂] (Ar' = 2,6-C₆H₃Me₂) with HSiMe₂Cl gives an isomeric structure [NbCp{η³-N(Ar')SiMe₂-H}-(PMe₃)₂(Cl)] **7** differing from **6** in that the phosphine rather than chloride lies *trans* to the co-ordinated Si–H bond. A preliminary X-ray study and large ¹J(Si–H) coupling constant of 116 Hz suggest that this compound is best described as an unstretched β-agostic (Si–H ··· M) d² silylamido complex. Reaction of the tantalum diphosphine compound [TaCp(NAr)(PMe₃)₂] with HSiMe₂Cl affords the d⁰ silylhydride derivative [TaCp(NAr)(H)(SiMe₂Cl)(PMe₃)] **8** which, according to an X-ray diffraction study and NMR data, has an interligand hypervalent interaction (IHI) between the silyl and hydride ligands. Reactions of **6** and **8** with Me₃SiX (X = I, OTf) lead to the corresponding iodido and triflate derivatives [NbCp{η³-N(Ar)SiMe₂-H}X(PMe₃)] (X = OTf **11** or I **12**) and [TaCp(NAr)(H)-(SiMe₂X)(PMe₃)] (X = OTf **14** or I **15**). Reaction of **8** with AgOTf gives [TaCp(NAr)(PMe₃)₂Cl]OTf **13**, the crystal structure of which has been determined. Density functional theory calculations on models of the compounds **6** and **7** showed that the experimental geometries are only correctly reproduced when the phosphine ligands are adequately modelled. The extent of oxidative addition of the Si–H bond to the metal in **6** mainly depends on the basicity of the phosphine ligand. With PH₃ in place of PMe₃ the calculated structures are better described as silanimine-hydrido derivatives. The formation of isomeric type **6** *versus* **7** is determined by an interplay of the steric and electronic effects of the ligand environment.

Introduction

The idea of non-classical interligand interactions was invoked about 30 years ago to describe the properties of what we now call σ-complexes like [MnCp(CO)₂(η²-H-SiR₃)].¹ This idea however did not become widely accepted until the class of agostic complexes **A** was clearly formulated in 1983, firstly for C–H bonds² (A, X = CR_n) and later for other elements.³ The experimental discovery by Kubas *et al.* of dihydrogen complexes,⁴ predicted theoretically by Bagatur'yants *et al.*,⁵ gave rise to intensive investigations of σ-complexes **B** (often also called η²-complexes⁷), which are now known for X = H,⁸ CR_n,⁹ SiR_n,⁷ GeR_n,¹⁰ SnR_n¹¹ and BR_n.¹² Examples of what can be regarded as a C–C → M and β-Si–C → M agostic interaction have also been reported.¹³

† Electronic supplementary information (ESI) available: selected bond distances and angles and a view of the preliminary X-ray structure of **7**. See <http://www.rsc.org/suppdata/dt/b1/b103362j/>



Interligand interactions in agostic and σ-complexes appear to have much in common, and initially were described by invoking the model originally developed to explain the bonding in diborane, *i.e.* in terms of three-centre two-electron (3c–2e) interactions M ← (X–Y).² Even now these systems are often quoted as having 3c–2e bonds. Later the importance of back-donation from the metal (in systems with dⁿ configurations where n > 1) for the stabilisation of a non-classical structure was realised¹⁴ and in a more refined way the bonding in agostic and σ-complexes is normally best described in terms of a donation from an X–Y σ bonding orbital to a vacant metal

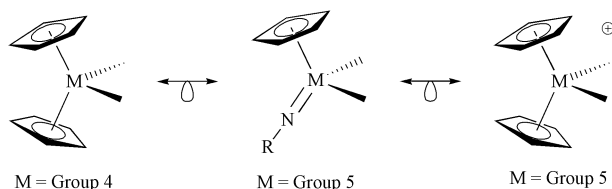
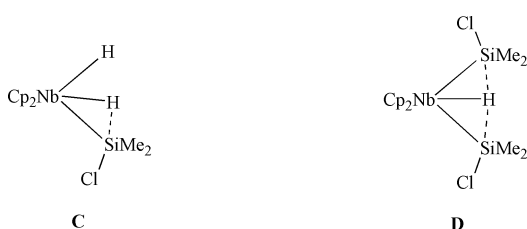


Fig. 1 Isolobal analogies between bis(cyclopentadienyl)- and cyclopentadienyl-imido-metal fragments for Groups 4 and 5.²⁴

orbital, supported by some back-donation from a filled metal d orbital to $\sigma^*(X-Y)$ (complete transfer of an electron pair to $\sigma^*(X-Y)$ breaks the $X-Y$ bond). Thus the term $3c-ne$ ($2 \leq n < 4$) bond appears to be more correct. This scheme is analogous to the Dewar–Chatt–Duncanson model for the bonding of olefins to transition metals.¹⁵ More recent theoretical and experimental studies showed that the α - and β -C–H \rightarrow M systems are different: the α -C–H \rightarrow M interaction mainly originates from an electronic reorganisation of the M–C bond upon tilting,¹⁶ whereas β -C–H \rightarrow M agostic systems mainly have β -C \cdots M interactions.¹⁷ Nevertheless, the bonding in β -Si–H \rightarrow M agostic silyl compounds¹⁸ is probably analogous to that in σ -complexes (*i.e.* a $3c-ne$ X–H \rightarrow M bond).

Nikonov *et al.* have recently identified a different kind of interligand interaction which to a considerable extent resembles the bonding in so-called hypervalent compounds like I_3^- , PCl_5 , *etc.*¹⁹ This non-classical interaction can occur in basic transition metal hydrides (in contrast to the often acidic hydrides involved in agostic and σ -complexation) and stems from a formal donation of the M–H bond electrons into an E–X σ^* antibonding orbital.²⁰ The term “interligand hypervalent interaction” (IHI) has been coined to describe this kind of interaction.^{20a} So far IHI has been observed only for silyl ligands²¹ (E = Si) bearing electron-withdrawing (and good leaving) groups X (X = F, Cl, Br, I, OTf) and were found in two forms: four-centre four-electron interactions M–H \rightarrow Si–X, which can be also described as three-centre four-electron interligand interactions ($3c-4e$) in the co-ordination sphere of a transition metal (C),^{20c-d} and six-centre six-electron interactions X–Si \leftarrow H(–M) \rightarrow Si–X (*i.e.* a five-centre six-electron interligand interaction ($5c-6e$) in the co-ordination sphere of a transition metal, D).^{20a-c} In the niobocene complexes C and D the IHI was investigated by means of X-ray^{20a-c} and neutron^{20e} diffraction experiments, NMR relaxation^{20e} and DFT calculations.^{20c,22} A β -IHI between a hydride and β -positioned silicon in a silylamide ligand has also been recently described.²³



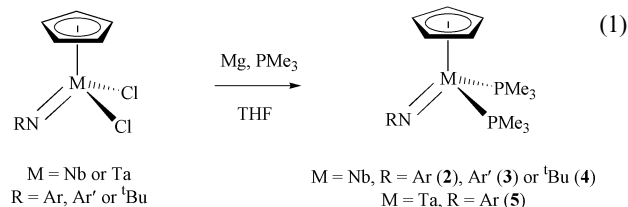
Interested in further studying non-classical interligand interactions, we set up a research programme focused on the preparation and investigation of silylhydride complexes having non-metallocene ligand environments.^{20d} In this paper we report our investigation of niobium and tantalum complexes with the cyclopentadienyl-imido ligand set which is related to the metallocene environment through the isolobal analogy²⁴ (Fig. 1). A preliminary account of this work has been published.²⁵

Results and discussion

Starting complexes

Group 5 diphosphine complexes $[MCp(NR)(PMe_3)_2]$ (M = Nb, Ta) seemed to be the natural choice of precursors to the target silane oxidative addition products $[MCp(NR)(SiR_2X)(H)(PR_3)]$

that are isolobal analogues of the non-classical niobocenes C and D. Gibson and Siemeling have reported that $[NbCp^*(NAr)(PMe_3)_2]$ ($Cp^* = \eta-C_5Me_5$; Ar = 2,6- $C_6H_3Pr_2$) can be easily prepared by magnesium reduction of $[NbCp^*(NAr)Cl_2]$ by analogy to the corresponding reduction of $[TiCp_2Cl_2]$ to give $[TiCp_2(PMe_3)_2]$.²⁶ While this work was in progress, Gibson *et al.* also reported the preparation of the complex $[NbCp(NC_6H_4^t-Bu-2)(PMe_3)_2]$.²⁷ We have synthesised a series of homologous diphosphine complexes of niobium and tantalum (2–5) having a cyclopentadienyl-imido ligand environment [eqn. (1)]. The



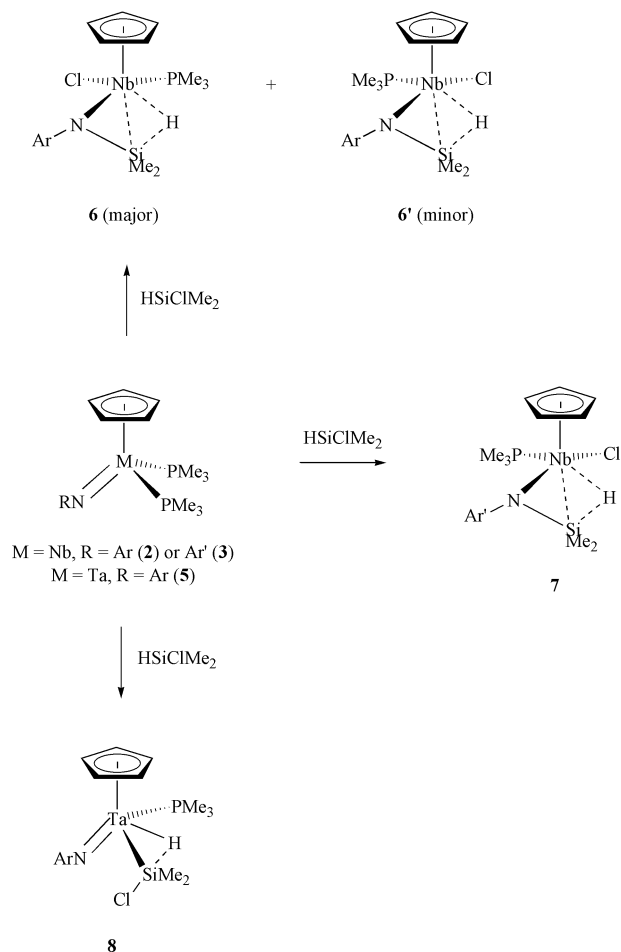
dichloride precursors $[MCp(NR)Cl_2]$ (M = Nb or Ta; R = ^tBu or Ar) have been described previously.^{24b,28} The new compound $[NbCp(NAr')Cl_2]$ (1, Ar' = 2,6- $C_6H_3Me_2$) was prepared by analogy with the literature method for $[NbCp(NAr)Cl_2]$.^{24b} Characterising data for the new compounds 1–5 are listed in the Experimental section; the data are analogous to those of the previously described Cp^* homologues and do not warrant further discussion.

It is known that $[NbCp^*(NAr)(PMe_3)_2]$ reacts with dihydrogen at 60 °C to give the dihydride $[NbCp^*(NAr)H_2(PMe_3)]$.²⁶ Because phosphine dissociation is the likely first step in any corresponding oxidative addition reaction of $[MCp(NR)(PMe_3)_2]$ with a silane $HSiR_3$ (to generate 16 electron intermediates $[MCp(NR)(PMe_3)]$ that would be amenable to an oxidative addition reaction) we therefore first studied the thermal stability of the complexes $[MCp(NR)(PMe_3)_2]$ 2–5 in the absence of any added substrate. The aryl substituted compounds 2 and 3 were found to be stable in C_6D_6 even after heating at 100 °C for several hours. In contrast, the *tert*-butylimido complex 4 is unstable and slowly decomposes at room temperature. Thus after being in C_6D_6 solution overnight at room temperature, the ¹H NMR spectrum of 4 showed the presence of another product having Cp, ^tBu and PMe_3 signals integrating in the relative ratios 5 : 9 : 9. However, this (presumably) monophosphine complex is itself unstable and cannot be isolated from the reaction mixture. Its structure (*e.g.*, dimeric *versus* monomeric) remains unclear.

Reactions of $[NbCp(NR)(PMe_3)_2]$ with silanes

In spite of its thermal stability, $[NbCp(NAr)(PMe_3)_2]$ 2 reacts smoothly with an excess of $HSiMe_2Cl$ overnight at room temperature to give the silylamido compound $[NbCp\{\eta^3-N(Ar)SiMe_2-H\}Cl(PMe_3)]$ 6 (Scheme 1). Compound 6 crystallises from pentane solution in the form of large dark green crystals in 84% isolated yield. Close examination of the ¹H NMR spectrum revealed the presence of two compounds (6 and 6') in the ratio 10 : 1. The non-classical structure of the main component was unequivocally supported by an X-ray diffraction study (*vide infra*). This complex has a formal four-leg piano-stool structure with a β -agostic Si–H bond as depicted in Scheme 1.

The minor component of the mixture (6' – Scheme 1) is believed to be an isomer of 6, having the phosphine ligand *trans* to Si–H and the Cl atom in a position *cis* to Si–H. In contrast to the high-field Nb–H resonance at -5.67 ppm in 6, the postulated isomer 6' displays a very different hydridic signal at -3.76 ppm. The difference in shift can be attributed to a different degree of Si–H and Nb–H interactions. The ¹H NMR spectrum of the mother liquor taken after crystallisation of 6 and 6' revealed a mixture, the main component of which (apart from



Scheme 1 Reactions of HSiMe_2 with $[\text{MCp}(\text{NR})(\text{PMe}_3)_2]$ ($M = \text{Nb}$ or Ta , $R = \text{Ar}$ or Ar').

the remaining **6** and **6'**) was a compound tentatively formulated as $[\text{NbCp}(\mu\text{-NAr})\text{Cl}]_2$ based on the similarity of the spectrum with its tantalum analogue (*vide infra* – **9**). Complex **6** is sufficiently stable at room temperature to allow work-up. However, it decomposes in solution over several weeks with the formation of $[\text{NbCp}(\mu\text{-NAr})\text{Cl}]_2$. A small quantity of another by-product crystallised in the form of small red crystals from the reaction mixture after prolonged standing (weeks) at room temperature. An X-ray diffraction study revealed this to be the known Nb(III) complex $[\text{NbCp}(\text{PMe}_3)_3\text{Cl}]_2$.²⁹

The $\nu(\text{Nb-H})$ IR band for **6** appears at 1620 cm^{-1} which is close to the typical region for $\nu(\text{Nb-H})$ in niobocene hydrides ($1650\text{--}1750\text{ cm}^{-1}$).³⁰ For comparison, uncoordinated Si-H bonds exhibit $\nu(\text{Si-H})$ bands at about 2100 cm^{-1} , whereas in the d^0 Si-H...M β -agostic systems of the type **A** this band appears at about 1800 cm^{-1} .^{3a-c} These IR data suggest a stretching of the Si-H bond in **6** upon complexation to metal. However, the observation of a large $^1J(\text{Si-H})$ coupling constant of 97 Hz reveals a direct bonding between silicon and hydride, and provides unambiguous support for the non-classical structure of **6**. The large $^1J(\text{Si-H})$ coupling constant in **6** comprehensively rules out its alternative description as a η^2 -silanimine-hydride complex of the type **E**. It is noteworthy, however, that this $^1J(\text{Si-H})$ is significantly diminished in comparison with the values observed for d^0 Si-H...M β -agostic systems [$^1J(\text{Si-H}) = 113\text{--}142\text{ Hz}$] of the type **F**.

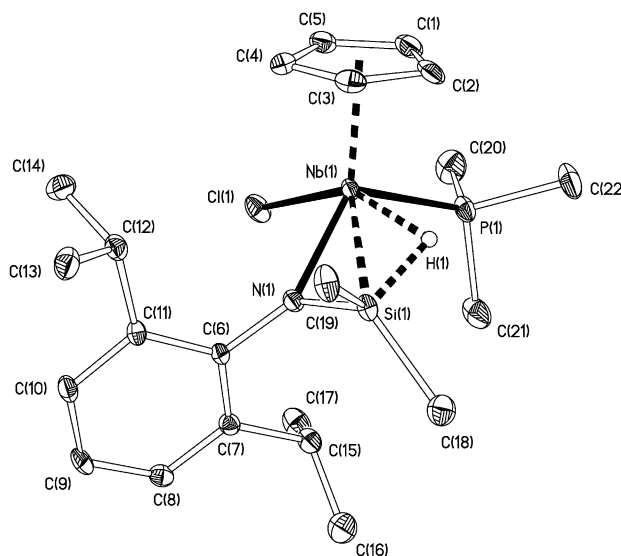


Fig. 2 Molecular structure of $[\text{NbCp}\{\eta^3\text{-N}(\text{Ar})\text{SiMe}_2\text{-H}\}\text{Cl}(\text{PMe}_3)]$ **6**. Displacement ellipsoids are drawn at the 30% probability level, except for H(1) which is shown as a sphere of arbitrary radius.

The arylimido compound $[\text{NbCp}(\text{NAr}')(\text{PMe}_3)_2]$ **3** reacts with HSiMe_2Cl in a similar way to $[\text{NbCp}(\text{NAr})(\text{PMe}_3)_2]$ **2**, giving the non-classical complex $[\text{NbCp}\{\eta^3\text{-N}(\text{Ar}')\text{SiMe}_2\text{-H}\}\text{Cl}(\text{PMe}_3)]$ **7** (Scheme 1). The structure of this complex was established by IR and NMR spectroscopy and a preliminary X-ray diffraction study (a view of the molecular structure along with selected bond lengths and angles are available as ESI†). In contrast to **6**, this compound exhibits only one detectable isomeric form. The hydride resonance of **7** was found at -3.41 ppm , very close to the Nb-H signal of the minor isomer of $[\text{NbCp}\{\eta^3\text{-N}(\text{Ar}')\text{SiMe}_2\text{-H}\}\text{Cl}(\text{PMe}_3)]$, namely **6'**, suggesting that they possess similar structures. This hydrogen shift is close to the typical region for classical niobocene hydrides, in contrast to the somewhat higher-field position observed for **6**. An upfield hydride resonance shift is often associated with a bridging position for a hydride ligand, which might suggest that **6** has a stronger non-classical Nb...H...Si interaction, while **6'** and **7** lie closer to the classical end of the spectrum of possible structures. However, the hydride resonance is also strongly influenced by the anisotropy of the ligand environment. For example the cyclopentadienyl-imido complex $[\text{NbCp}^*(\text{NAr})(\text{H})_2(\text{PMe}_3)]$ exhibits a hydride signal at 3.36 ppm ,²⁶ whereas in $[\text{TaCp}^*(\text{NAr})(\text{H})\{\text{Si}(\text{SiMe}_3)_3\}]$ a surprisingly low-field shifted hydride resonance at 21.49 ppm was found.³¹

The uncertainty concerning the extent of the Nb...H...Si interactions in **6'** and **7** was resolved by the observation of an increased $^1J(\text{Si-H})$ coupling constant of 116 Hz in **7** (the corresponding value for **6** is 97 Hz). This value is well within the range of values usually observed in unstretched d^0 Si-H...M β -agostic structures, and is just slightly less than usually observed (*ca.* 150 Hz) for classical Si-H bonds. This implies that the co-ordination of the Si-H bond in **7** is weaker than that in **6**, which has been further supported by DFT calculations (*vide infra*).

The X-ray diffraction study of **7**† unequivocally established the positions of the non-hydrogen atoms and revealed the difference between the two isomeric forms of **6** and **7**. That is to say, in **7** (and presumably in **6'**) the phosphine ligand lies *trans* to the Si-H bond, while the Cl atom is in a mutually *cis* position. Unfortunately, a discussion of any further details of the structure is not possible because of the very poor quality of the crystal (see Experimental section).

The molecular structure of $[\text{NbCp}\{\eta^3\text{-N}(\text{Ar})\text{SiMe}_2\text{-H}\}\text{Cl}(\text{PMe}_3)]$ **6** as determined by X-ray diffraction study is shown in Fig. 2, and selected bond lengths and angles are collected in Table 1. It has a formal four-leg piano-stool structure if

Table 1 Selected bond distances (Å) and angles (°) for [NbCp{η³-N(Ar)SiMe₂-H}Cl(PMe₃)] **6**

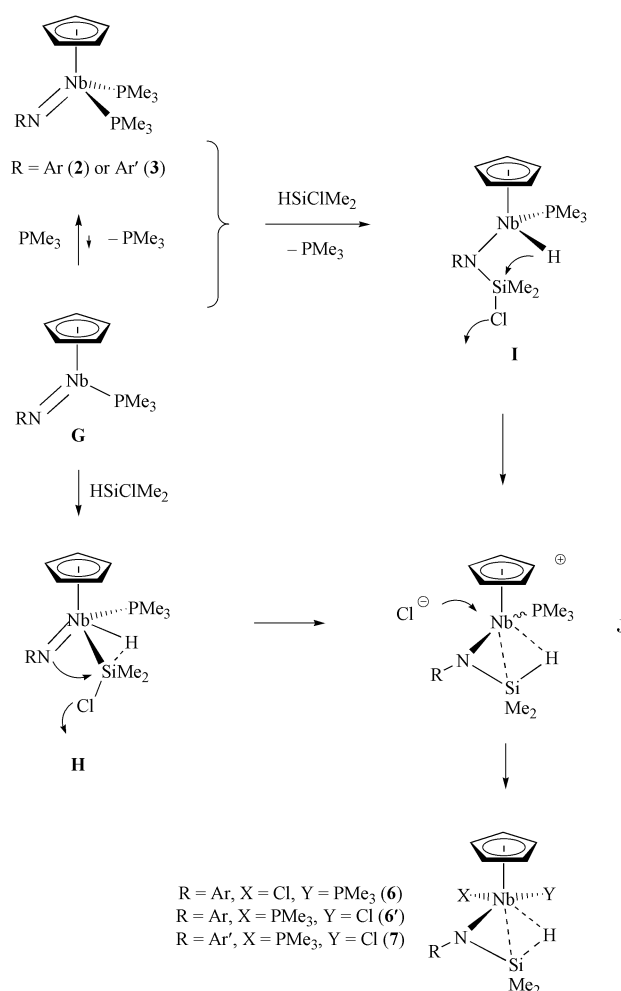
Nb(1)–N(1)	2.051(4)	Nb(1)–H(1)	1.91(5)
Nb(1)–P(1)	2.552(1)	Si(1)–H(1)	1.52(5)
Nb(1)–Si(1)	2.646(1)	Si(1)–N(1)	1.704(4)
Nb(1)–Cl(1)	2.497(1)		
Nb(1)–N(1)–Si(1)	89.09(16)	Si(1)–Nb(1)–Cl(1)	123.42(5)
Si(1)–Nb(1)–P(1)	109.37(5)		

one considers the η³-co-ordinated N(Ar)SiMe₂-H ligand as occupying two co-ordination sites. The co-ordination sphere of niobium is completed by Cp, Cl and PMe₃ ligands, with the chlorine *trans* to the β-agostic Si–H bond. The Nb⋯H⋯Si bridging hydrogen atom, H(1), was located from a Fourier difference map and refined isotropically to Nb–H and Si–H distances of 1.91(5) and 1.52(5) Å, respectively. This Nb–H bond length is significantly longer than normally observed for terminal Nb–H bonds (range *ca.* 1.60–1.81 Å, depending on the experimental method^{30b,c,32,33}), but is noticeably shorter than the corresponding distance in the d⁰ β-agostic Si–H complexes (2.3–2.5 Å).³ The observed Si–H contact is longer than values previously reported for free or β-agostic Si–H bonds (range *ca.* 1.42–1.50 Å).³ It is also instructive to consider the Nb(1)–N(1)–Si(1) angle of 89.1(2)° in **6**. This is comparable with the M–N–Si angles found previously for silanimine compounds [86.1(1) and 89.1(2)° for two examples³⁴] and is significantly smaller than the corresponding values for β-agostic (Si–H⋯M) silylamine (of the type **F**) complexes [range 95.1(1)–103.4(1)° for four examples^{3a–c}]. However, a description of **6** as a classical η²-silanimine-hydride complex (of the type **E**) is not consistent with the Nb(1)–Si(1) distance of 2.646(1) Å. Thus, despite the presence of an electron-withdrawing nitrogen substituent at Si, Nb(1)–Si(1) falls within the range of Nb–Si bond lengths observed [2.613–2.669(3) Å] for niobium silyl derivatives having only alkyl and aryl groups on Si.^{20c,30b,35} By way of contrast, authentic silanimine complexes feature M–Si bonds that are considerably shorter than in related alkylsilyl derivatives.^{34a}

Therefore the elongated Nb–H and Si–H bonds, contracted Nb–Si–N angles, diminished ¹J(Si–H), along with other NMR and IR data suggest that the bonding in **6** is intermediate between a β-agostic d² silylamine (**F**) and a d⁰ silanimine-hydride (**E**) structure.

Reaction of the alkylimido precursor [NbCp(NBu^t)(PMe₃)₂] (**7**) with HSiMe₂Cl proceeds in a very different manner to that for **5** and **6**. Combination of these reagents results in a mixture, the main component of which was isolated from ether and found by ¹H NMR (CDCl₃) to be the known dimer [NbCp-(μ-NBu^t)Cl]₂.²⁸ A very weak hydride signal at –6.22 ppm which could be attributed to a compound structurally analogous to **6** or **7** was also observed in the ¹H NMR (C₆D₆) spectrum of the reaction mixture. Therefore the result of an interaction of diphosphine complexes [NbCp(NR)(PMe₃)₂] with HSiMe₂Cl depends critically on the identity of the R group of the imido moiety.

The mechanism of formation of **6** (and **6'**) and **7** is of interest and Scheme 2 proposes two feasible alternatives. In principle, the reactions would proceed *via* the formal oxidative addition of HSiMe₂Cl to the metal centre of an intermediate monophosphine complex [NbCp(NR)(PMe₃)] **G** which might exist in a small amount (not observable by ¹H NMR) in equilibrium with [NbCp(NR)(PMe₃)₂] (Scheme 2). The subsequent first-formed product of this addition (**H**) is analogous to the tantalum compound **8** discussed below which has been isolated and fully characterised. Intramolecular attack of the imido nitrogen lone pair on the Si–Cl bond of **H** would generate the ion pair **J**; this in turn can collapse to form **6**, **6'** or **7** with Cl or PMe₃ *trans* to the Si–H bond as required. Alternatively these products could result from Si–H addition across the reactive RN=Nb bond. Such Si–H additions have been previously described by

**Scheme 2** Two alternative mechanisms for the formation of [NbCp{η³-N(R)SiMe₂-H}Cl(PMe₃)] (R = Ar **6**, **6'** or Ar' **7**).

Tilley *et al.*^{23,31b} Such a reaction could in principle occur *via* the 18 electron **5** or **6** or the monophosphine **G**. A similar sequence of possible steps proceeding (*via* **I** or its bis(phosphine) analogue) again through ion pair **J** would lead to the observed products (Scheme 2). At this time we are not able to distinguish between the two main mechanistic alternatives (*i.e.*, initial attack at Nb or at RN=Nb).

We have examined the reaction of [NbCp(NAr)(PMe₃)₂] **2** with other silanes and chlorosilanes. No reaction of ClHSi^tPr₂ with **2** was observed, which suggests a sensitivity to steric factors. In addition, neither ClSiMe₃ nor Cl₂SiMe₂ react with **2** at room temperature. A reaction was observed only after heating the reaction mixture at 100 °C for some hours, but the products remain unknown.

Surprisingly, no HSiMe₂Ph addition to **2** occurs even after overnight heating at 100 °C. Attempted reaction of **2** with HSiMe₂Ph in the presence of BH₃·THF as a phosphine sponge resulted in a mixture of products. A separate experiment showed that the same mixture emerges after the reaction of **2** with BH₃·THF in the absence of a silane. This lack of reactivity suggests that the classical complex [NbCp(NAr)(H)-(SiMe₂Ph)(PMe₃)] (analogous to **H** in Scheme 2 with Ph in place of Si-bound Cl) may not exist.

Reactions of [TaCp(NR)(PMe₃)₂] with silanes

The reaction of the tantalum complex [TaCp(NAr)(PMe₃)₂] **5** with HSiClMe₂ (Scheme 1) gives a dramatically different type of complex to those formed (**6**, **7**) in the reactions of the niobium compounds **2** and **3**. The product [TaCp(NAr)(H)-(SiMe₂Cl)(PMe₃)] (**8**) is a d⁰ complex and was obtained in 61% isolated yield. It possesses a different type of non-classical

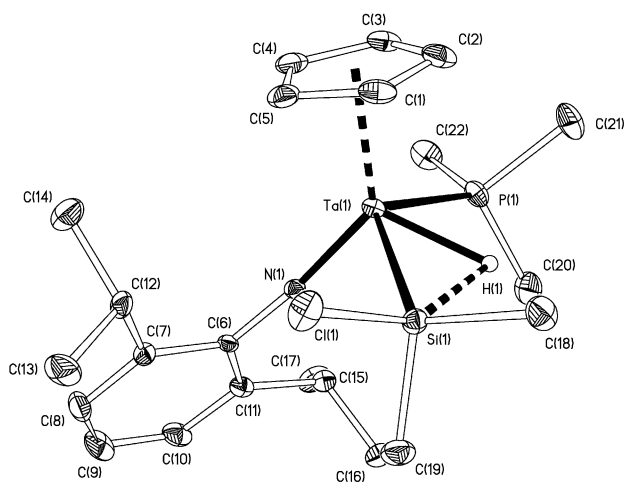


Fig. 3 Molecular structure of [TaCp(NAr)(H)(SiMe₂Cl)(PMe₃)] **8**. Displacement ellipsoids are drawn at the 25% probability level, except for H(1) which is shown as a sphere of arbitrary radius. H atoms except H(1) excluded for clarity.

Table 2 Selected bond distances (Å) and angles (°) for [TaCp(NAr)(H)(SiMe₂Cl)(PMe₃)] **8**

Ta(1)–N(1)	1.821(4)	Ta(1)–H(1)	1.6(1)
Ta(1)–P(1)	2.550(1)	Si(1)···H(1)	2.3(1)
Ta(1)–Si(1)	2.574(1)	P(1)···H(1)	2.3(1)
Cl(1)–Si(1)	2.177(2)		
P(1)–Ta(1)–Si(1)	120.63(5)	Cl(1)–Si(1)–Ta(1)	112.05(7)

M···H···Si interaction. The compound **8** shows well-defined sets of signals for the Cp, NAr, SiMe₂ and PMe₃ ligands in its NMR spectra. The Ta–H resonance appears as a doublet [²J(H–P) = 64.2 Hz] at 5.13 ppm; the unusually low-field shift may be attributed to the anisotropy of the double bond of the imido ligand. The compound **8** is a rare example of a stable transition metal hydride complex supported by an imido ligand.^{26,36} Other relevant examples are the Nb complex [NbCp*(NAr)(PMe₃)₂]²⁶ and the Ta complexes [TaCp*(N-Bu^t)(PMe₃)(H)(CH₃)]^{36a} and [TaCp*(NAr)(H){Si(SiMe₃)₃}].³¹

The X-ray solid state structure of **8** is shown in Fig. 3 and Table 2 lists selected bond lengths and angles. The solid state structure is consistent with the solution NMR data and shows that the Ta-bound hydride, Si and P atoms all lie in the “bisecting plane” between the Cp and NAr ligands. This is consistent with the isolobal analogy between [MCp₂X₃] and [MCp(NAr)(X)₂L] where X and L are 1- and 2-electron donor ligands, respectively.²⁴ The silicon-bound chlorine atom lies approximately *trans* to H(1) and its maximum deviation from the calculated {Ta(1),P(1),H(1),Si(1),Cl(1)} least-squares plane is 0.13 Å.

The geometry at Ta in **8** closely resembles that of Nb in the non-classical complexes [NbCp₂(X)(H)(SiMe₂Cl)] (X = H **C** or SiMe₂Cl **D**),²⁰ assuming that the arylimido group occupies the co-ordination site of one of the Cp rings. Analogous approximately *trans* positions of apical Si–Cl bond and metal-bound H in respect to the MMe₂ unit formally comprising an equatorial plane were previously observed in **C** and **D**. Recent experimental and theoretical studies have shown that comparatively short M–Si and long Si–Cl bonds are associated with interligand hypervalent interactions (IHIs) between the Si and H ligands.²⁰ The Si–Cl bond length of 2.177(2) Å in **8** is one of the longest reported for [ML_n(SiR₂Cl)] (R = alkyl, aryl) complexes.³⁷ Furthermore, it is comparable to that found in the non-classical complex **C** [Si–Cl = 2.170(2) Å] but significantly longer than that of **D** [Si–Cl = 2.163(1) Å]. The Ta–Si bond of 2.574(1) Å in **8** is the shortest reported to date [average 2.638, range 2.611–2.671 Å for six Ta(+5) non-disordered observa-

tions],³⁸ and is comparable to the Nb–Si bonds in **C** and **D** 2.579(2) and 2.597(1) Å, respectively; these in turn are shorter than in other silyl derivatives of niobocene.³⁰

The question naturally arises as to whether **8** is a thermodynamically stable form or a kinetic product on the way to a formal d² structure like **6** (just as **H** may be an intermediate in the formation of **6** and **7** – Scheme 2). Complex **8** seems to be indefinitely stable at room temperature as a solid. However, an initially pure C₆D₆ solution kept at room temperature in ambient light for weeks showed the steady formation of another mono phosphine-hydride compound, the ¹H NMR spectrum of which showed a hydride ligand signal as a doublet at 10.26 ppm (²J(H–P) = 69.6 Hz). The low-field shift of this hydride signal relative to the corresponding signal in **8** (5.13 ppm, ²J(H–P) = 64.2 Hz) can be attributed either to a different anisotropy (for example due to a lateral position of this ligand in comparison with the central one in **8**) or to the presence of an electron-withdrawing chlorine ligand directly bound to the tantalum if a compound like [Cp(NAr)Ta(Cl)(H)(PMe₃)] is formed. Surprisingly, under moderate heating (50 °C, several hours) **8** does not show signs of decomposition. However, after 3 days heating at 92 °C it decomposes to give specifically the chloro-complex [TaCp(μ-NAr)Cl]₂ (**9**). Free H₂SiMe₂ and PMe₃ were observed in the ¹H NMR spectrum when this reaction was carried out in a sealed NMR tube. No signals attributable to a structure like **6** were observed. The presumably dimeric structure of **9** is consistent with that found in the solid state for related compounds³⁹ such as [NbCp(μ-NAr)Me]₂.^{39a}

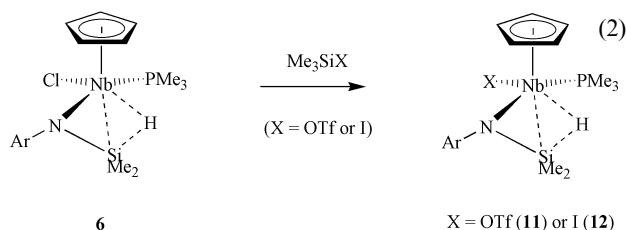
As for [NbCp(NAr)(PMe₃)₂] **2**, no reaction of [TaCp(NAr)(PMe₃)₂] **5** with HSiMe₂Ph occurs at room temperature, and a mixture is observed after thermolysis at 100 °C. Alkylation of **8** with MeLi in an NMR tube scale reaction does produce the compound [TaCp(NAr)(H)(SiMe₃)(PMe₃)] **10** in quantitative yield. However, although the NMR tube scale reaction was very clean, attempts to isolate **10** on a preparative scale were unsuccessful. This compound is fairly stable at room temperature although it slowly decomposes on heating at 92 °C with elimination of HSiMe₃ (detected in the ¹H NMR spectrum) producing a mixture of Cp-containing compounds. In contrast to the corresponding niobium chemistry, [TaCp(NAr)(PMe₃)₂] **5** was not identified among the products.

Functionalisation reactions of [NbCp{η³-N(Ar)SiMe₂-H}-(Cl)(PMe₃)] **6** and [TaCp(NAr)(H)(SiMe₂Cl)(PMe₃)] **8**

The degree of interligand interactions in **6** and **8** can depend on the identity of the substituents at Nb and Si, respectively. It is of interest therefore to study their functionalised derivatives, namely the products of formal substitution of Cl in both compounds for other groups. We initially focused on the synthesis of other halogen- and triflate-substituted complexes. This reaction of [NbCp{η³-N(Ar)SiMe₂-H}-(Cl)(PMe₃)] **6** with BF₃·Et₂O gives an intractable mixture of products, whereas rapid reduction of Ag⁺ with the production of silver metal is observed on reaction with AgPF₆. In neither case were signals assignable to the desired product [NbCp{η³-N(Ar)SiMe₂-H}-(F)(PMe₃)] observed in the NMR spectra. Silver is also formed on treatment of **6** with AgOTf, but the main component of the soluble part of the mixture is the substitution product [NbCp{η³-N(Ar)SiMe₂-H}-(OTf)(PMe₃)] **11**.

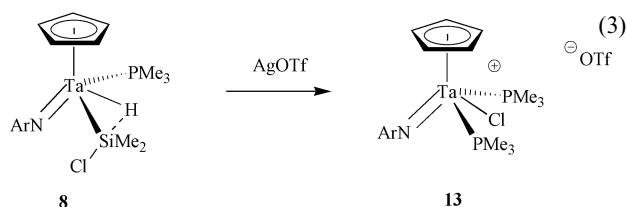
A cleaner route to **11** is *via* the reaction of **6** with Me₃SiOTf. Only one isomer, having a hydride ligand signal at –7.00 ppm, was formed. The analogous reaction with Me₃SiI gave a high yield of the iodo derivative [NbCp{η³-N(Ar)SiMe₂-H}-(I)(PMe₃)] **12** which, like **6**, was obtained as a mixture of two isomers in the ratio 8 : 3. The structures of **11** and **12** [eqn. (2)] were established by NMR spectroscopy, the main characteristics of the NMR spectra being analogous to those of **6**.

We also attempted the direct alkylation of **6**. Addition of one equivalent of MeLi resulted initially in a mixture containing



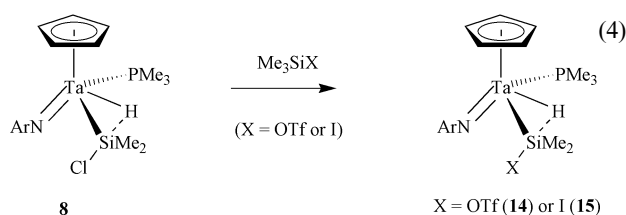
three Cp-containing compounds. One of these, formed in about 30% yield, was identified (by integration of the ^1H NMR spectrum), as the diphosphine complex $[\text{NbCp}(\text{NAr})(\text{PMe}_3)_2]$ **2**. Two other main products each contained only one phosphine ligand since their Cp signals appear as doublets at 5.38 ppm and 5.10 ppm. A hydride signal, corresponding to the Cp signal at 5.38 ppm (in a *ca.* 1 : 5 ratio by integration), was found at -5.6 ppm. This hydride-containing compound decomposes on standing while signals due to **2** and other decomposition products grow. The main silane product identified by ^1H NMR is HSiMe_3 . These observations suggest that alkylation of **6** initially affords a hydride complex which then eliminates HSiMe_3 probably giving the unstable monophosphine $[\text{NbCp}(\text{NAr})(\text{PMe}_3)]$ **G**. Disproportionation of the latter presumably results in **2** and a mixture of decomposition products.

As for **6**, the reaction of the tantalum compound **8** with AgOTf in ether mainly results in the reduction of Ag^+ to silver metal. However, a yellow oil was formed after solvent removal from the soluble part and yellow needles of $[\text{TaCp}(\text{NAr})(\text{PMe}_3)_2\text{Cl}]\text{OTf}$ **13** [eqn. (3)] crystallised from the mother liquor.



The identity of this compound was established by X-ray structure analysis (see below).

Reactions of **8** with Me_3SiOTf and Me_3SiI give the Si-triflate- and -iodo-substituted derivatives $[\text{TaCp}(\text{NAr})(\text{SiMe}_2\text{OTf})(\text{H})(\text{PMe}_3)]$ **14** and $[\text{TaCp}(\text{NAr})(\text{SiMe}_2\text{I})(\text{H})(\text{PMe}_3)]$ **15**, respectively, in good yields [eqn. (4)]. The structures of these



compounds were established by their NMR spectra which are very similar to those of **8**. Attempts to grow X-ray quality crystals of **11**, **12**, **14** and **15** were unsuccessful.

The molecular structure of the cationic part of **13** is shown in Fig. 4 and selected molecular parameters are collected in Table 3. The geometry around tantalum can be described as a four-legged piano-stool, or alternatively as a tri-substituted Cp-imido complex. Among eight other structurally characterised tri-substituted Cp-imido complexes, five are trichlorides of molybdenum and tungsten and their methylated derivatives,⁴⁰ and two examples are mono phosphine adducts of niobium dichlorides $[\text{NbCp}(\text{NR})(\text{PMe}_3)\text{Cl}_2]$.^{24a,41} The closest analogue is the zirconium complex $[\text{ZrCp}'(\text{NAr})(\text{py})_2\text{Cl}]$ ($\text{Cp}' = \text{C}_5\text{H}_4\text{Me}$) which contains a chlorine atom between the two 2-electron donors.⁴² The Ta=N bond length of 1.809(6) Å in $[\text{Ta}(\text{NAr})\text{Cl}(\text{PMe}_3)_2]^+$ is at the long end of the known range for a Ta=

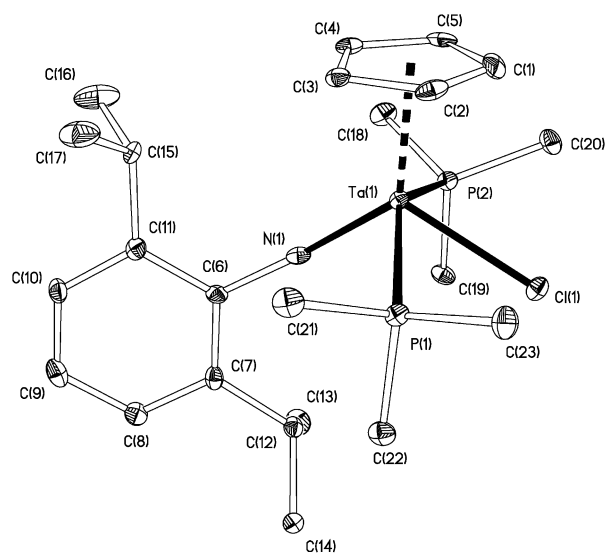


Fig. 4 The molecular structure of the cationic part of $[\text{CpTa}(\text{NAr})(\text{Cl})(\text{PMe}_3)_2]\text{OTf}$ **13**. Displacement ellipsoids are drawn at the 25% probability level. H atoms are excluded for clarity.

Table 3 Selected bond distances (Å) and angles ($^\circ$) for the cationic part of $[\text{TaCp}(\text{NAr})(\text{PMe}_3)_2\text{Cl}]\text{OTf}$ **13**

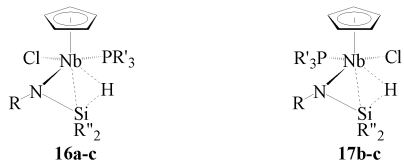
Ta(1)–N(1)	1.809(6)	Ta(1)–P(2)	2.621(2)
Ta(1)–P(1)	2.607(2)	Ta(1)–Cl(1)	2.458(2)
N(1)–Ta(1)–P(1)	85.7(2)	P(1)–Ta(1)–P(2)	145.86(6)
N(1)–Ta(1)–P(2)	92.8(2)	Cl(1)–Ta(1)–P(2)	75.06(6)
N(1)–Ta(1)–Cl(1)	115.9(2)	Cl(1)–Ta(1)–P(1)	75.05(6)

N_{imido} bond in a cyclopentadienyl-imido ligand environment (range 1.780–1.800 Å for five known examples). The Ta–P bonds of 2.607(2) and 2.621(2) Å are comparable with Nb– PMe_3 bond lengths observed in related niobium Cp-imido compounds 2.528–2.604(3) Å.^{24b,27,43} The Ta–Cl bond of 2.458(2) Å can be compared with the Nb–Cl bonds in $[\text{NbCp}(\text{NAr})\text{Cl}_2(\text{PMe}_3)]$ (2.499(2) and 2.494(2) Å)^{24a} but is noticeably longer than in other chloro-substituted Cp-imido complexes of tantalum such as $[\text{TaCp}^*(\text{NAr})\text{Cl}_2]$ ^{24b} and $[\text{TaCp}^*(\text{NAr}')\text{Cl}_2]$ ⁴⁴ (2.345(2), 2.331(2) and 2.326(2) Å, respectively) and longer than the corresponding bonds in $[\text{NbCp}(\text{NR})\text{Cl}_2]$ ^{24b,27} (range 2.338–2.355(1) Å). Taking into account that the radii of tantalum and niobium are very close, the elongation of the Ta–Cl bond relative to the disubstituted systems is apparently caused by the increased steric congestion around the Ta centre, whereas shortening in comparison with $[\text{NbCp}(\text{NAr})\text{Cl}_2(\text{PMe}_3)]$ can be accounted for by the positive charge of the complex.

Computational studies

There is a growing number of successful applications of theoretical methods used to describe the non-classical structures of transition metal complexes.⁴⁵ The purpose of the current study was (i) to establish the hydride ligand position in models of the real compounds **6** and **7**, (ii) to determine the nature of the Si–H and Si–M interactions in these species and (iii) to understand the factors controlling the formation of the two isomeric forms **16** (as found for **6**) and **17** (as found for **6'** and **7**). Density functional theory (DFT) calculations can provide a means for predicting the location of hydrides and for studying interligand and metal-to-ligand interactions.^{45a} As relatively large molecular systems are usually of interest, the problem of adequate modelling arises. For reasons of computational economy it is normal practice to model some or all of the ligand substituents by hydrogen atoms. However, we found that this approach did not work well for the compounds under consideration here. Indeed there are previous examples of the serious dependence

of computational results on the level of simplification.^{45a,g} Three different types of ligand substitution in the model complexes **16** and **17** were examined in the current study. The first has all of the substituents at the nitrogen (R), phosphorus (R') and silicon (R'') atoms modelled by hydrogen atoms. The second has a phenyl substituent at nitrogen but hydrogens at phosphorus and silicon. The most advanced, third model has a phenyl substituent at nitrogen as well as methyl-substituted phosphorus and silicon atoms. In further discussions these models will be designated by the suffixes **a**, **b** and **c**, respectively.



(a) R = R' = R'' = H; (b) R = Ph, R' = R'' = H; (c) R = Ph, R' = R'' = Me

Our calculations show that adequate modelling of the phosphine ligand has the greatest impact on the results. Thus the full geometry optimisation of **16a** (R = R' = R'' = H) afforded a structure far away from that of **6** (R = Ar, R' = R'' = Me). The most noticeable discrepancy was in the Si–H distances: 2.37 Å calculated for **16a** versus 1.52(5) Å observed for **6**. We next turned to Ph as a more realistic substituent (R in **16**) at nitrogen. However, a full geometry optimisation of **16b** (R = Ph) resulted in only a minor improvement of the DFT structure in comparison with the experiment. Thus the Si–H distance contracted only to 2.26 Å and a Nb–H distance of 1.78 Å was found. The Nb–Si distance slightly contracted to 2.56 Å (*cf.* 2.57 Å in **16a**) versus 2.646(1) Å in **6**. Overall, the discrepancy between the observed (**6**) and calculated (**16b**) structures was still too great.

Introduction of the methyl substituents at the phosphorus (R') and silicon (R'') atoms (**16c**) resulted in significant improvements in the Nb–H and Si–H distances (1.87 and 1.73 Å, respectively) which now agreed much better with the experimental values (1.91(5) and 1.52(5) Å). The good agreement between the more sophisticated model **16c** and the real complex **6** helps validate the observed position of the hydride ligand in the X-ray structure of the latter. It is noteworthy that the Nb–H and Si–H bond distances calculated for **16c** are very close to values observed in the previously communicated calculation in which only the hydride position was optimised (Nb–H and Si–H bond distances of 1.93 and 1.77 Å, respectively).²⁵ The validity of this partial optimisation (model **16d**) is therefore also supported by the new and complete calculation. Note also that the electronic structure of **16d** features a metal-based HOMO that is well set up for back-donation into the Si–H σ^* antibonding orbital. Thus the real compounds **6** and **7** (as represented by the model compound **17c** – *vide infra*) formally have a d², Nb(III) centre and they are best described by the β -agostic silylamine description **F**. The basic electronic structures of the complexes **6** and **7** are related to those of the four-legged piano-stool type [MCpL₄] which are well known.^{46,47}

The most important structural parameters obtained for **16a–c** and **17b–c** are collected in Table 4 where corresponding X-ray values of **6** are given for comparison. As can be seen, on comparing **16a** to **16c**, the N–Si distance contracts approaching the experimental value. This shortening of the N–Si bond length parallels lengthening of the Nb–H, Nb–Si and Nb–N distances and thus can be viewed as supporting a transition from a formal silanimido-hydride structure (**16a**) to a β -agostic silylamine structure (**16c**). It is also interesting to consider the variations of the Nb–Cl and Nb–P distances. Not surprisingly, the introduction of electron-donating methyl substituents in **16c** results in a considerable decrease in the Nb–P bond length from 2.63 (in **16b**) to 2.56 Å (**16c**) which is very close to the experimental value of 2.552(1) Å in **6**. This process is accompanied by a

Table 4 Selected calculated and observed parameters for complex [NbCp{ η^3 -N(Ar)SiMe₂-H}Cl(PMe₃)] **6** and the models [NbCp{ η^3 -N(R)SiR''₂-H}Cl(PR' ₃)] **16a–d** and **17b–c**^a

Parameter	Calculated values						X-Ray 6
	16a	16b	16c	16d ^b	17b	17c	
Nb–Si	2.57	2.56	2.58	—	2.57	2.77	2.646(2)
Nb–N	1.99	2.03	2.05	—	2.02	2.06	2.051(4)
N–Si	1.78	1.83	1.75	—	1.81	1.75	1.704(4)
Nb–Cl	2.56	2.60	2.59	—	2.55	2.55	2.497(1)
Nb–P	2.58	2.63	2.56	—	2.77	2.57	2.552(1)
Si–H	2.37	2.26	1.73	1.77	2.36	1.57	1.52(5)
Nb–H	1.84	1.78	1.87	1.93	1.75	2.06	1.91(5)

^a For models carrying suffix **a**: R = R' = R'' = H; those with the suffix **b**: R = Ph, R' = R'' = H; those with the suffix **c**: R = Ph, R' = R'' = Me.
^b DFT optimisation of the hydride ligand only, the rest of the structure is “frozen” in the X-ray geometry.²⁵

minor shortening of the Nb–Cl bond, which lies *trans* to the Si–H bond, from 2.60 (in **16b**) to 2.59 Å in **16c** [although this value is still somewhat longer than found in the X-ray structure of **6** (2.497(1) Å)]. Although the shortening of Nb–Cl from **16b** to **16c** is at first sight opposite to what might be predicted on the basis of steric factors alone, it probably follows from the concomitant lengthening of the Nb–H bond in **16c** and hence a reduced *trans* influence on the Nb–Cl bond approximately *trans* to it.

To gain a similar insight into the isomeric compound **7** we first carried out a geometry optimisation of the model **17b** (R = Ph, R' = R'' = H). This has a PH₃ ligand *trans* to the hydride, and a Cl atom *trans* to the N–Si unit. A greater *trans* influence of the hydride relative to the N–Si moiety is clearly observed on comparison of the two isomers **16b** and **17b** optimised at the same level of modelling (Table 4). Thus, the Nb–P bond elongates (from 2.63 to 2.77 Å) and the Nb–Cl bond shortens (from 2.60 to 2.55 Å) on going from **16b** to the isomeric **17b**. Despite the *trans* position of the phosphine ligand relative to hydride, the Si–H bond in **17b** is lengthened (2.36 Å) compared to that in **16b** (2.26 Å) while the Nb–H bond is slightly shorter (by 0.03 Å) in **17b**. The differences in the Nb–H and Si–H distances for **16b** and **17b** are relatively minor and suggest that in this system the Cl[−] and PH₃ ligands have comparable *trans* influences and σ donor properties;⁴⁸ in addition, the weakly 3p π \rightarrow 4d π donating ability of Cl might be slightly better in **17b** (shorter Nb–Cl bond) than in **16b**. This would destabilise the d² HOMO of **17b** and have a small enhancing effect on the Nb to Si–H σ^* back-donation. While this is probably not a very important effect, it is in agreement with the Si–H (longer in **17b**) and Nb–H (shorter in **17b**) distances.

Energetically, the isomer **16b** is only 1.1 kcal mol^{−1} more stable than **17b**. However, for the more sophisticated models **16c** and **17c** (R = Ph, R' = R'' = Me) the stability order is reversed, with compound **17c** being more stable than **16c** by 2.5 kcal mol^{−1}. In these two systems we found a surprising inversion of the relative bond distance values. Thus in **17c** the Si–H bond shortens substantially to 1.57 Å with concomitant elongation of the Nb–H bond to 2.06 Å, thus resulting in a structure with a *weaker* β -Si–H \rightarrow M agostic interaction than that in **16c**. These computational results are in excellent agreement with the Si–H coupling constant data for **7** [¹J(Si–H) = 116 Hz] and **6** [¹J(Si–H) = 97 Hz]. Thus, at the most sophisticated level of modelling (in terms of N-, P- and Si-substituents) the DFT calculations correctly reproduce the key experimental observations, namely that (i) the energies of the two isomers are apparently rather close (recall that [NbCp{ η^3 -N(Ar)SiMe₂-H}Cl(PMe₃)] exists as two isomers, **6** and **6'**) and (ii) that in the absence of steric congestion (*e.g.*, Ar' in place of Ar) the structural type **17** (as is found for complex **7**) appears to be more stable than **16**.

Table 5 NBO's between atoms of the first coordination sphere of niobium in the models **16c** and **17c**

Natural bond	16c			17c		
	Occupation ^a	Energy/ E_h^a	Composition of bonding NBO	Occupation ^a	Energy/ E_h^a	Composition of bonding NBO
Nb–P	1.905/0.287	−0.403/+0.002	28% Nb [s(17%) d(83%)] 72% P [s(34%) p(66%)]	1.917/0.306	−0.398/+0.017	29% Nb [s(18%) d(82%)] 71% P [s(35%) p(65%)]
Nb–N	1.845/0.286	−0.253/−0.068	23% Nb [s(4%) d(96%)] 77% N [s(3%) p(97%)]	1.862/0.263	−0.305/−0.062	20% Nb [s(3%) d(97%)] 80% N [s(11%) p(89%)]
Nb–N				1.658/0.525	−0.489/−0.038	9% Nb [s(7%) d(93%)] 91% N [s(42%) p(58%)]
Nb–H(<i>hydride</i>)	1.543/0.311	−0.256/+0.005	37% Nb [s(10%) d(90%)] 63% H [s(100%)]			
Si–H(<i>hydride</i>)				1.713/0.056	−0.348/+0.208	36% Si [s(23%) p(76%) d(1%)] 64% H [s(100%)]

^a Bonding and antibonding NBOs are separated by a forward slash.

Table 6 Values and the changes (Δ) in the interatomic distances, Mulliken orbital populations (condensed to atoms), Wiberg indices, and overlap-weighted NAO bond orders between **16c** and **17c**

Bond	Interatomic distances (Å)			Mulliken orbital populations			Wiberg indices			NAO bond orders		
	16c	17c	Δ	16c	17c	Δ	16c	17c	Δ	16c	17c	Δ
Nb–P	2.557	2.568	0.01	0.124	0.150	0.03	0.662	0.651	−0.01	0.544	0.546	0.00
Nb–Cl	2.588	2.554	−0.03	0.160	0.160	0.00	0.608	0.701	0.09	0.486	0.541	0.06
Nb–N	2.056	2.060	0.00	0.044	0.040	0.00	0.960	0.900	−0.06	0.628	0.629	0.00
Nb–Si	2.578	2.768	0.19	0.039	0.008	−0.03	0.371	0.167	−0.20	0.384	0.251	−0.13
Nb–H(<i>hydride</i>)	1.869	2.057	0.19	0.189	0.144	−0.05	0.412	0.231	−0.18	0.368	0.267	−0.10
Si–H(<i>hydride</i>)	1.730	1.567	−0.16	0.080	0.213	0.13	0.433	0.634	0.20	0.488	0.629	0.14
Si–N	1.755	1.753	0.00	0.348	0.367	0.02	0.672	0.672	0.00	0.705	0.707	0.00

The interligand bonding in **16c** and **17c** was further elucidated by NBO (natural bond orbital) analysis (Table 5). Within the standard thresholds the NBO analysis identified a Nb–H bond in **16c** whereas no Si–H bond was detected. In contrast, in **17c** a Si–H bond, but no Nb–H bond, was present. Both bonds are very electron deficient which reflects their delocalised nature. These data are in accord with the calculated Mulliken orbital populations, NAO (natural atomic orbital) bond orders and WB (Wiberg bond) indices (Table 6). Thus the WB index is higher for the Nb–H bond in **16c** (0.412) than for that in **17c** (0.231), whereas the reverse order is observed for the Si–H bond (0.433 in **16c** versus 0.634 in **17c**). All these data show that the Si–H bond is in a greater degree of oxidative addition to the metal centre in **16c** than in **17c**, and that in the latter the Si–H bonding predominates over the Nb–H bonding. The parameters for the other groups in **16c** and **17c** do not differ that much.

The DFT predictions (Table 4) that both of the PMe_3 -substituted models **16c** and **17c** have stronger Si–H interactions (and longer Nb–H distances) than in their PH_3 -substituted homologues (**16b** and **17b**) is at first sight counter-intuitive. In principle, one might have expected that increasing the basicity of the phosphine ligand, and hence the electron-richness of the metal, would lead to more advanced Si–H bond cleavage since this represents (in the limit) a formal oxidative addition to the metal. This apparently paradoxical result is accounted for as follows.

The dramatic increase in the Si–H interaction upon going from **17b** to **17c** can be understood by considering the *trans* influence of the ligand *trans* to the Si–H bond. The usual order of the *trans* influence is $\text{PR}'_3 > \text{Cl}^-$,⁴⁸ but the exact influence exerted by PR'_3 ligands depends on the basicity of the phosphine, which in turn depends on the nature of the R' groups. We have already noted that in **16b** and **17b** the *trans* influence of PH_3 does not differ much from that of Cl^- . However, introducing the methyl group on phosphorus (*trans* to Nb–H–Si) in **17c** increases the σ donor ability of phosphine and its *trans* influence. Thus the overall ligand-to-metal bonding is opti-

mised by forming a stronger Nb–P (2.57 Å) bond than in **17b** and the accompanying lengthening of the Nb–H bond (2.06 Å) is compensated for by a pronounced shortening of the Si–H bond (1.57 Å). Thus the different extents of Nb–H and Si–H interactions in **17b** and **17c** are due to the very different basicity of the phosphine ligand in the two models. In effect, on going from **17b** to **17c**, the tension generated by having two strong *trans* influence ligands (*i.e.* H and PR'_3) opposite each other results in stronger Nb–P bonding at the expense of Nb–H bonding, but the loss of Nb–H bonding is attenuated by Si–H bond formation.

The strengthening of the Si–H interaction on going from **16b** to **16c** (PR'_3 *cis* to Nb–H–Si) can be explained similarly in terms of a *cis*-labilising effect which is known to be of secondary significance in comparison with the *trans* influence.⁴⁸ Therefore increased basicity of the phosphine also labilises the Nb–H interaction, but not that much as when PR'_3 is in a *trans* position (as in **17c**). For this reason **16c** has a stronger Si–H bond than in **16b** but weaker than in **17c**. The slight shortening of the Nb–Cl bond on going from **16b** to **16c** is most likely attributed to the diminished Nb–H interaction *trans* to it.

The observation that the sterically more hindered **6** has a greater degree of Si–H addition to the metal than **7** appears to be paradoxical. However, comparison of the calculated structures of **16c** and **17c** shows that different degree of Si–H oxidative addition hardly affects the Nb–N distance and hence the degree of repulsion of the R group on N from the Cp ring. The driving force for the preference of the isomer **6** versus **6'** therefore appears to be the repulsion of the R from the *cis*-ligand. In this context it is obvious that a bulkier R group on N will favour the chloride rather than the larger PR'_3 in the *cis*-position, *i.e.* the formation of the structural type **16** versus **17**. When the importance of the steric factor diminishes, as in **7**, the structural type **17** starts to dominate, which is in accord with our calculations (**17c** more stable than **16c**).

The question why the tantalum complex **8** prefers a d^0 structure is still open and will be the subject of further studies. However, it appears that one possibility is the greater

propensity of tantalum to exist in the oxidation state +5. In contrast, the niobium compounds **6** and **7** have a partially occupied 4d level due to the incomplete back-donation to the Si–H σ^* antibonding orbital.

Experimental

General methods and instrumentation

All manipulations of air- and/or moisture-sensitive compounds were carried out under an atmosphere of dinitrogen or argon using standard Schlenk-line or dry-box techniques at room temperature unless stated otherwise. All protio-solvents and commercially available reagents were pre-dried over activated molecular sieves and refluxed over an appropriate drying agent under an atmosphere of dinitrogen and collected by distillation. NMR solvents for air- and/or moisture-sensitive compounds were dried over appropriate agents, distilled under reduced pressure and stored under N₂ in J. Young ampoules. NMR samples of air- and moisture-sensitive compounds were prepared in the dry-box in 5 mm Wilmad tubes, equipped with a Young's Teflon valve.

¹H, ¹³C and ²⁹Si spectra were recorded on Varian Unity Plus 500, Varian Mercury V × 300 or Bruker 300 spectrometers and referenced internally to residual protio-solvents (¹H) or solvent (¹³C) resonances. Chemical shifts are reported relative to tetramethylsilane ($\delta = 0$ ppm) in δ (ppm) with coupling constants in Hertz. IR spectra were obtained as Nujol mulls with a FTIR Perkin-Elmer 1600 series spectrometer. HSiMe₂Cl, Me₃SiI, Me₃SiOTf and anilines were obtained from Sigma-Aldrich. PMe₃,⁴⁹ [MCpCl₄] (M = Nb or Ta),⁵⁰ [MCp(NAr)(Cl)₂] (M = Nb or Ta)^{24b} and [MCp(NBu^t)Cl₂]³⁹ (M = Nb, Ta) were prepared according to the literature methods. A modified method for the preparation of [TaCp(NAr)Cl₂]^{24b} is given below.

Preparation of [TaCp(NAr)Cl₂]

This known compound was prepared by an adaptation of the literature method^{24b} via the reaction of [TaCpCl₄] but with one equivalent of Me₃SiNHAr in the presence of 2,6-lutidine. Yield 51%. ¹H NMR (C₆D₆): 7.13 (d, *J*(H–H) = 7.7 Hz, 2 H, C₆H₃), 6.82 (t, *J*(H–H) = 7.7 Hz, 2 H, C₆H₃), 5.76 (s, 5 H, Cp), 3.71 (sept, *J*(H–H) = 6.9 Hz, 2 H, CHMe₂), 1.28 (d, *J*(H–H) = 6.9 Hz, 12 H, CHMe₂). ¹³C-¹H NMR (C₆D₆): 150.3 (CN), 145.5 (CCHMe₂), 125.6, 122.1 (C₆H₃), 112.2 (Cp), 28.0 (CHMe₂), 24.1 (CHMe₂).

Preparation of [NbCp(NAr')Cl₂] (**1**)

This new compound was prepared by analogy with the literature method developed for [NbCp(NAr)Cl₂]^{24b} via the reaction of [NbCpCl₄] with one equivalent of Me₃SiNHAr' in the presence of 2,6-lutidine. Yield 34%.

¹H NMR (CDCl₃): 6.93 (d, *J*(H–H) = 7.2 Hz, 2 H, C₆H₃), 6.81 (t, *J*(H–H) = 7.2 Hz, 1 H, C₆H₃), 6.56 (s, 5 H, Cp), 2.41 (s, 6 H, Me). ¹³C-¹H NMR (CDCl₃): 134.0, 127.5 (CH of C₆H₃), 113.8 (Cp), 19.0 (Me). C₁₃H₁₄NNbCl₂ (348.07): calcd C 44.86, H 4.05, N 4.02; found C 45.44, H 4.39, N 3.78%.

Preparation of [NbCp(NAr)(PMe₃)₂] (**2**)

0.46 g (6 mmol) of PMe₃ was added to a mixture of 0.343 g (14.1 mmol) of Mg and 1.150 g (2.845 mmol) of [NbCp(NAr)(Cl)₂] in 15 mL of THF. After 20 min the resultant yellow mixture turned darker. The mixture was stirred overnight. Volatiles were removed *in vacuo* and the resultant mixture was extracted with hexane and filtered to give a dark green-brown solution. Hexane removal gave a dark green-brown crystalline solid. Yield: 1.144 g (83%).

¹H NMR (C₆D₆): 7.15 (d, *J*(H–H) = 6.8 Hz, 2 H, C₆H₃), 7.02 (t, *J*(H–H) = 6.8 Hz, 1 H, C₆H₃), 5.05 (s, 5 H, Cp), 4.27 (sept,

J(H–H) = 6.9 Hz, 2 H, CHMe₂), 1.27 (d, *J*(H–H) = 6.9 Hz, 12 H, CHMe₂), 1.09 (d, *J*(H–P) = 6.0 Hz, 18 H, PMe₃). ¹³C-¹H NMR (C₆D₆): 141.0, 122.5, 120.1 (C₆H₃), 92.8 (Cp), 27.3 (CHMe₂), 24.3 (CHMe₂), 24.2 (PMe₃). ³¹P-¹H NMR (C₆D₆): 20.6 (br). C₂₃H₄₀NNbP₂ (485.43): calcd C 56.91, H 8.31, N 2.98; found C 55.28, H 8.00, N 2.91%.

Preparation of [NbCp(NAr')(PMe₃)₂] (**3**)

This was prepared in an analogous manner to **2** from 0.668 g (1.912 mmol) of [NbCp(NAr')(Cl)₂]. Yield: 0.585 g (71%).

¹H NMR (C₆D₆): 7.17 (d, *J*(H–H) = 7.3 Hz, 2 H, C₆H₃), 6.88 (t, *J*(H–H) = 7.3 Hz, 1 H, C₆H₃), 5.04 (s, 5 H, Cp), 2.43 (s, 6 H, Me), 1.08 (br s, 18 H, PMe₃). ¹³C-¹H NMR (C₆D₆): 130.0, 118.5, (C₆H₃), 92.6 (Cp), 24.2 (br, PMe₃), 21.6 (Me). Satisfactory elemental analysis could not be obtained for this very air-sensitive material.

Preparation of [NbCp(NBu^t)(PMe₃)₂] (**4**)

This was prepared in an analogous manner to **2** from 1.37 g (4.56 mmol) of [NbCp(NBu^t)(Cl)₂]. Yield: 0.868 g (51%).

¹H NMR (C₆D₆): 5.10 (s, 5 H, Cp), 1.40 (s, 9 H, CMe₃), 1.17 (d, *J*(H–P) = 7.0 Hz, 18 H, PMe₃). ¹³C-¹H NMR (C₆D₆): 91.5 (Cp), 68.0 (CMe₃), 26.5 (d, *J*(P–C) = 18.4 Hz, PMe₃). Satisfactory elemental analysis could not be obtained for this very air-sensitive material.

Preparation of [TaCp(NAr)(PMe₃)₂] (**5**)

A solution of 1.180 g (2.07 mmol) of [TaCp(NAr)Cl₂] in 30 mL of THF was added to a mixture of 0.250 g (10.3 mmol) of Mg and 0.50 mL (4.83 mmol) of PMe₃. In some seconds the mixture turned purple. After 40 h stirring at room temperature volatiles were removed *in vacuo* and the resultant mixture was extracted with hexane (3 × 30 mL) and filtered to give a dark green-brown solution. Hexane removal gave a dark green-brown crystalline solid. Yield: 1.03 g (87%).

¹H NMR (C₆D₆): 7.16 (d, *J*(H–H) = 6.8 Hz, 2 H, C₆H₃), 7.08 (t, *J*(H–H) = 7.3 Hz, 1 H, C₆H₃), 4.93 (t, *J*(P–H) = 1.3 Hz, 5 H, Cp), 4.22 (sept, *J*(H–H) = 7.0 Hz, 2 H, CHMe₂), 1.28 (d, *J*(H–H) = 7.0 Hz, 12 H, CHMe₂), 1.24 (vt, *J*(H–P) = 3.6 Hz, 18 H, PMe₃). ¹³C-¹H NMR (C₆D₆): 140.1, 122.5, 119.4 (C₆H₃), 90.5 (Cp), 27.3 (CHMe₂), 24.1 (CHMe₂), 27.9 (vt, *J*(P–C) = 11.2 Hz, PMe₃). ³¹P-¹H NMR (C₆D₆): 20.6 (br). Satisfactory elemental analysis could not be obtained for this very air-sensitive material.

Preparation of [NbCp{ η^3 -N(Ar)SiMe₂-H}(Cl)(PMe₃)] (**6**)

To a suspension of [NbCp(NAr)(PMe₃)₂] (1.459 g, 3.09 mmol) in pentane (15 mL) was added HSiClMe₂ (1.3 mL, excess). The mixture was kept for 5 days to afford large dark green crystals. These were filtered off, washed with cold pentane and dried *in vacuo*. Yield: 1.280 g (84%). Solution was reduced in volume to 5 mL and a second crop of **6** (0.200 g) crystallised after 3 days. Total yield: 97%.

IR (Nujol): 1620 cm⁻¹ ν (Nb–H).

6: ¹H NMR (C₆D₆): 7.25 (d, *J*(H–H) = 7.3 Hz, 1 H, C₆H₃), 7.24 (d, *J*(H–H) = 7.2 Hz, 1 H, C₆H₃), 7.17 (m, 1 H, C₆H₃), 4.67 (d, *J*(H–P) = 1.7 Hz, 5 H, Cp), 3.33 (sept, *J* = 6.7 Hz, 1 H, CHMe₂), 2.37 (sept, *J* = 6.8 Hz, 1 H, CHMe₂), 1.50 (d, *J* = 6.7 Hz, 3 H, CHMe₂), 1.32 (overlapping 2 × d, *J* = 6.8 Hz, 6 H, 2 × CHMe₂), 1.14 (d, *J* = 6.8 Hz, 3 H, CHMe₂), 0.96 (d, *J*(H–P) = 7.8 Hz, 9 H, PMe₃), 0.31 (d, *J*(H–P) = 2.0 Hz, 3 H, SiMe₂), 0.22 (d, *J* = 0.9 Hz, 3 H, SiMe₂), –5.67 (s, 1 H, Nb–H). ¹³C-¹H NMR (C₆D₆): 148.0, 140.9, 123.5, 123.26, 123.1 (C₆H₃), 93.6 (Cp), 27.6, 27.4, 26.9, 25.68, 25.1, 24.5, 18.0 (d, *J*(C–P) = 23.9 Hz, PMe₃), 3.7 (Si–Me), 2.3 (Si–Me). ³¹P-¹H NMR (C₆D₆): 11.5. ²⁹Si-¹H selective NMR (C₆D₆): –52.1 (*J*(H–Si) = 97 Hz).

6': 4.80 (s, 5 H, Cp), 1.67 (d, *J* = 6.5 Hz, 3 H, CHMe₂), 0.61 (d, *J*(H–P) = 6.1 Hz, 9 H, PMe₃), 0.28 (s, 3 H, SiMe₂), –0.10 (s,

3 H, SiMe₂), -3.76 (s, 1 H, Nb-H). ¹³C-¹H NMR (C₆D₆): 96.0 (s, Cp). Other signals are too weak or obscured by the signals of **6**.

C₂₂H₃₈ClNNbPSi (503.95): calcd C 51.90, H 7.60, N 2.78; found C 51.9, H 7.71, N 2.60%.

Preparation of [NbCp{η³-N(Ar')SiMe₂-H}(Cl)(PMe₃)] (7)

To a suspension of [NbCp(NAr')(PMe₃)₂] (0.219 g, 0.51 mmol) in pentane (15 mL) was added HSiClMe₂ (0.3 mL, excess). The mixture was kept at room temperature for 9 days to afford large dark green crystals. These were filtered off, washed with cold pentane and dried *in vacuo*. Yield: 0.180 g (79%). IR (Nujol): 1670.0 cm⁻¹ ν(Nb-H). ¹H NMR (C₆D₆): 7.11 (d, *J*(H-H) = 7.2 Hz, 1 H, C₆H₃), 6.92 (m, 1 H, C₆H₃), 6.87 (d, *J*(H-H) = 7.2 Hz, 1 H, C₆H₃), 4.76 (s, 5 H, Cp), 2.87 (s, 3 H, Me), 1.14 (s, 3 H, Me), 0.64 (d, *J*(H-P) = 7.2 Hz, 9 H, PMe₃), 0.51 (s, 3 H, SiMe₂), -0.23 (s, 3 H, SiMe₂), -3.41 (s, 1 H, Nb-H). ¹³C-¹H NMR (C₆D₆): 129.6, 128.7, 122.51 (C₆H₃), 95.7 (Cp), 20.8, 19.4 (Si-Me), 15.7 (d, *J*(C-P) = 18.1 Hz, PMe₃), 1.07 (Si-Me). ³¹P-¹H NMR (C₆D₆): 1.94. ²⁹Si-¹H selective NMR (C₆H₆): -68.0 (¹*J*(H-Si) = 116 Hz). C₁₈H₃₀ClNNbPSi (447.861): calcd C 48.27, H 6.75, N 3.13; found C 48.1, H 6.71, N 3.15%.

Preparation of [TaCp(NAr)(H)(SiMe₂Cl)(PMe₃)] (8)

To a solution of [TaCp(NAr)(PMe₃)₂] (1.03 g, 1.10 mmol) in pentane (30 mL) was added HClSiMe₂ (0.5 mL). After 14 h a light pink precipitate formed which was filtered off and dried *in vacuo*. Yield: 0.651 g (61%). IR (Nujol): 1736 cm⁻¹ ν(Ta-H). ¹H NMR (C₆D₆): 7.10 (d, *J*(H-H) = 7.8 Hz, 2 H, C₆H₃), 6.98 (t, *J*(H-H) = 7.8 Hz, 1 H, C₆H₃), 5.52 (d, *J*(H-P) = 1.5 Hz, 5 H, Cp), 5.13 (d, *J*(H-P) = 64.2 Hz, 1 H, Ta-H), 4.04 (sept, *J*(H-H) = 6.9 Hz, 2 H, CHMe₂), 1.27 (d, *J*(H-H) = 6.9 Hz, 6 H, CHMe₂), 1.23 (d, *J*(H-H) = 6.9 Hz, 6 H, CHMe₂), 1.23 (s, 3 H, SiMe₂), 0.95 (s, 3 H, SiMe₂), 0.90 (d, *J*(H-P) = 8.5 Hz, 9 H, PMe₃). ¹³C-¹H NMR (C₆D₆): 152.9, 142.9, 122.7 (C₆H₃), 100.3 (Cp), 27.1, 24.4 (d, *J*(C-P) = 12.8 Hz, PMe₃), 20.1 (Si-Me), 19.7 (Si-Me), 15.7, 14.8. ³¹P-¹H NMR (C₆D₆): -4.28. ²⁹Si-¹H selective NMR (C₆D₆): 91.7 (¹*J*(H-Si) = 33.3 Hz). C₂₂H₃₈ClNPSiTa (591.99): calcd C 44.63, H 6.47, N 2.37; found C 44.72, H 6.46, N 2.30%.

Preparation of [CpTa(μ-NAr)Cl]₂ (9)

A solution of 0.52 g (0.99 mmol) of **8** in 15 mL of toluene was refluxed under reduced pressure in a sealed, partially evacuated ampoule for 3 days at 92 °C. The solution was filtered and the volatiles removed under reduced pressure to give **9**. Yield: 0.220 g (49%).

¹H NMR (C₆D₆): 7.17 (d, *J*(H-H) = 7.8 Hz, 1 H, C₆H₃), 7.12-7.05 (m, C₆H₃), 5.77 (s, 5 H, Cp), 2.77 (sept, *J*(H-H) = 6.7 Hz, 2 H, CHMe₂), 1.30 (d, *J*(H-H) = 6.6 Hz, 2 H, CHMe₂), 1.17 (d, *J*(H-H) = 6.7 Hz, 2 H, CHMe₂). ¹³C-¹H NMR (C₆D₆): 170.4, 139.8, 125.3, 124.8 (C₆H₃), 109.3 (Cp), 27.3, 27.1, 25.4. C₁₇H₁₇Cl₂N₂Ta (456.78): calcd C 44.70, H 4.85, N 3.07; found C 42.25, H 5.14, N 2.81%.

Preparation of [TaCp(NAr)(H)(SiMe₃)(PMe₃)] (10)

In an NMR tube a solution of **8** in C₆D₆ was treated with MeLi (1.4 M in Et₂O) to form immediately **10** in quantitative yield by ¹H NMR integration.

¹H NMR (C₆D₆): 7.10 (d, *J*(H-H) = 7.7 Hz, 2 H, C₆H₃), 6.99 (t, *J*(H-H) = 7.7 Hz, 1 H, C₆H₃), 5.90 (s, 1 H, Ta-H), 5.37 (d, *J*(H-P) = 1.4 Hz, 5 H, Cp), 4.05 (sept, *J*(H-H) = 6.9 Hz, 2 H, CHMe₂), 1.27 (d, *J*(H-H) = 6.9 Hz, 6 H, CHMe₂), 1.21 (d, *J*(H-H) = 6.8 Hz, 6 H, CHMe₂), 0.96 (d, *J*(H-P) = 8.4 Hz, 9 H, PMe₃), 0.77 (s, 9 H, SiMe₃). ¹³C-¹H NMR (C₆D₆): 142.5, 122.6, 121.8 (C₆H₃), 98.8 (Cp), 26.9, 24.4, 24.2, 20.5 (d, *J*(C-P) = 29.5 Hz, PMe₃), 10.6 (Si-Me). ³¹P-¹H NMR (C₆D₆): -4.00.

Preparation of [NbCp{η³-N(Ar)SiMe₂-H}(OTf)(PMe₃)] (11)

0.5 mL (2.76 mmol) of Me₃SiOTf was added to 40 mL of toluene solution of **6** (1.024 g, 2.03 mmol). After 2 days at room temperature the solution was filtered and stripped of volatiles to give **11** as a dark green solid. Yield: 0.404 g (24%).

IR (Nujol): 1621.0 cm⁻¹ ν(Nb-H). ¹H NMR (C₆D₆): 7.21 (m, 1 H, C₆H₃), 7.10 (m, 2 H, C₆H₃), 4.90 (d, *J*(H-P) = 1.5 Hz, 5 H, Cp), 3.41 (d, *J*(H-H) = 7.0 Hz, 3 H, CHMe₂), 1.54 (d, *J*(H-H) = 7.0 Hz, 3 H, CHMe₂), 1.24 (d, *J*(H-H) = 7.0 Hz, 3 H, CHMe₂), 1.16 (d, *J*(H-H) = 7.0 Hz, 3 H, CHMe₂), 1.00 (d, *J*(H-P) = 8 Hz, 9 H, PMe₃), 0.94 (d, *J*(H-H) = 7.0 Hz, 3 H, CHMe₂), 0.33 (s, 3 H, SiMe₂), 0.10 (s, 3 H, SiMe₂), -6.96 (bs, 1 H, Nb-H). ³¹P-¹H NMR (C₆D₆): 10.9. ¹⁹F NMR (C₆D₆): -78.3. Satisfactory elemental analysis could not be obtained and attempted recrystallisation resulted in decomposition.

Preparation of [NbCp{η³-N(Ar)SiMe₂-H}(I)(PMe₃)] (12)

0.3 mL (2.11 mmol) of ISiMe₃ was added to 15 mL of toluene solution of **6** (0.375 g, 0.74 mmol). After 24 h at room temperature the volatiles were removed under reduced pressure to give a dark violet solid. Yield: 0.330 g (74%).

IR (Nujol): 1622.0 cm⁻¹ ν(Nb-H).

Isomer **12**: ¹H NMR (C₆D₆): 7.22 (m, C₆H₃), 7.00 (m, C₆H₃), 4.64 (d, *J*(H-P) = 1.8 Hz, 5 H, Cp), 3.26 (sept, *J*(H-H) = 6.9 Hz, 1 H, CHMe₂), 2.16 (sept, *J*(H-H) = 6.6 Hz, 1 H, CHMe₂), 1.58 (d, *J*(H-H) = 6.9 Hz, 3 H, CHMe₂), 1.42 (d, *J*(H-H) = 6.9 Hz, 3 H, CHMe₂), 1.28 (d, *J*(H-H) = 6.6 Hz, 3 H, CHMe₂), 1.14 (d, *J*(H-H) = 6.9 Hz, 3 H, CHMe₂), 1.03 (d, *J*(H-P) = 7.5 Hz, 9 H, PMe₃), 0.31 (d, *J*(H-P) = 2.4 Hz, 3 H, SiMe₂), 0.16 (d, *J*(H-P) = 2.4 Hz, 3 H, SiMe₂), -6.30 (br s, 1 H, Nb-H). ¹³C-¹H NMR (C₆D₆): 139.1, 129.3, 125.6, 123.9 (C₆H₃), 92.8 (Cp), 27.8, 27.4, 26.5, 26.0, 25.4, 22.7, 19.5 (d, *J*(C-P) = 24.6 Hz, PMe₃), 2.8, 1.9 (Si-Me).

Isomer **12'**: ¹H NMR (C₆D₆): 4.72 (d, *J*(H-P) = 2.4 Hz, 5 H, Cp), -4.10 (br s, 1 H, Nb-H). ¹³C-¹H NMR (C₆D₆): 94.5 (Cp). Other signals are too weak or obscured by the signals of **12**. Satisfactory elemental analysis could not be obtained.

Reaction of [TaCp(NAr)(H)(SiMe₂Cl)(PMe₃)] (8) with AgOTf to give [TaCp(NAr)(PMe₃)₂Cl]OTf (13) and [TaCp(NAr)(H)(SiMe₂OTf)(PMe₃)] (14)

AgOTf (0.067 g, 0.26 mmol) in diethyl ether (15 mL) was added to a solution of **8** (0.153 g, 0.26 mmol) also in diethyl ether (10 mL). A colour change quickly occurred and a black deposit was steadily formed. After 14 h some yellow crystals which grew on the walls were isolated manually. The solution was filtered and pumped off to give a yellow oil. ¹H NMR analysis of the oil (C₆D₆) showed the formation of [TaCp(NAr)(H)(SiMe₂OTf)(PMe₃)] **14** in ca. 30% yield (by integration of the spectrum) along with a mixture of at least three other products. The yellow crystals were of the compound [TaCp(NAr)(PMe₃)₂Cl]OTf (**13**). Insufficient quantities of **13** were isolated for additional analysis and its composition was unambiguously determined by an X-ray structure determination.

Preparation of [TaCp(NAr)(H)(SiMe₂OTf)(PMe₃)] (14)

0.3 mL (1.66 mmol) of Me₃SiOTf was added to a solution of 0.345 g (0.655 mmol) of **8** in 15 mL of toluene at room temperature. After stirring overnight in the dark the solution was filtered and volatiles were removed *in vacuo* affording 0.303 g (72%) of oily powder which was pure by NMR. IR (Nujol): 1626.0 cm⁻¹ ν(Ta-H). ¹H NMR (C₆D₆): 7.05 (d, *J*(H-H) = 7.2 Hz, 2 H, C₆H₃), 6.98 (t, *J*(H-H) = 7.1 Hz, 1 H, C₆H₃), 5.51 (d, *J*(H-P) = 1.5 Hz, 5 H, Cp), 4.32 (d, *J*(H-P) = 61.8 Hz, 1 H, Ta-H), 3.84 (sept, *J*(H-H) = 6.9 Hz, 2 H, CHMe₂), 1.24 (d, *J*(H-H) = 7.2 Hz, 6 H, CHMe₂), 1.19 (d, *J*(H-H) = 7.2 Hz, 6 H, CHMe₂), 1.06 (s, 3 H, SiMe₂), 0.88 (s, 3 H, SiMe₂), 0.82 (d, *J*(H-

Table 7 X-Ray data collection and processing parameters for [NbCp{ η^3 -N(Ar)SiMe₂-H}Cl(PMe₃)] **6**, [TaCp(NAr)(H)(SiMe₂Cl)(PMe₃)] **8** and [CpTa(NAr)(Cl)(PMe₃)₂]OTf **13**

	6	8	13
Formula	C ₂₂ H ₃₈ ClNNbPSi	C ₂₂ H ₃₈ ClNPSiTa	C ₂₄ H ₄₀ ClF ₃ NOP ₂ STa
Formula weight	503.95	591.00	757.97
Crystal system	monoclinic	monoclinic	triclinic
Space group	C2/c	P2 ₁ /c	P $\bar{1}$
<i>a</i> /Å	31.391(6)	15.893(1)	11.224(2)
<i>b</i> /Å	10.150(2)	9.092(1)	11.281(2)
<i>c</i> /Å	16.945(3)	19.136(2)	13.562(3)
α /°	—	—	100.71(3)
β /°	111.30(3)	112.568(3)	104.08(3)
γ /°	—	—	106.70(3)
<i>V</i> /Å ³	5030(2)	2553.5(4)	1533.5(5)
<i>Z</i>	8	4	2
μ (Mo-K α)/mm ⁻¹	0.704	0.453	3.887
Total reflections	4813	23837	11041
Observed reflections	3557 [<i>I</i> > 2 σ (<i>I</i>)]	4115 [<i>I</i> > 3 σ (<i>I</i>)]	4416 [<i>I</i> > 2 σ (<i>I</i>)]
<i>R</i> , ^a <i>R</i> _w , ^b or <i>wR</i> ₂ , ^c	0.050, 0.103 [<i>I</i> > 2 σ (<i>I</i>)]	0.030, 0.035 [<i>I</i> > 3 σ (<i>I</i>)]	0.0537, 0.0746 [<i>I</i> > 2 σ (<i>I</i>)]
<i>wR</i> ₂ , ^c (all data)	0.1152	—	0.0870

$$^a R_1 = \sum(|F_o| - |F_c|)/\sum|F_o|, ^b R_w = \{\sum w(|F_o| - |F_c|)^2/\sum(w|F_o|)^2\}^{1/2}, ^c wR_2 = \{\sum w(F_o^2 - F_c^2)^2/\sum(w(F_o^2))^2\}^{1/2}.$$

P) = 8.7 Hz, 9 H, PMe₃). ¹³C-¹H} NMR (C₆D₆): 139.1, 129.3, 125.6 (C₆H₃), 92.8 (Cp), 27.8, 27.4, 25.4, 22.7, 19.5 (d, J (C–P) = 24.6 Hz, PMe₃), 2.8, 1.9(Si–Me). ³¹P-¹H} NMR (C₆D₆): –2.93. Satisfactory elemental analysis could not be obtained.

Preparation of [CpTa(NAr)(H)(SiMe₂I)(PMe₃)] (**15**)

To 10 mL of toluene solution of **8** (0.359 g, 0.68 mmol) was added 0.3 mL (2.11 mmol) of ISiMe₃. The solution was kept 2 days in the dark, then filtered and stripped of solvents to give a yellow-brown oily compound which was pure by NMR. Yield: 0.357 g (77%).

IR (Nujol): 2093.0 cm⁻¹ ν (Ta–H). ¹H NMR (C₆D₆): 7.19–7.02 (m, C₆H₃), 5.90 (half of doublet, 0.5 H, Ta–H), 5.54 (br s, 5 H, Cp), 3.83 (sept, J(H–H) = 6.5 Hz, 2 H, CHMe₂), 1.34 (d, J(H–H) = 6.5 Hz, 6 H, CHMe₂), 1.26 (s, 3 H, SiMe₂), 1.18 (d, J(H–H) = 6.5 Hz, 6 H, CHMe₂), 0.43 (d, J(H–H) = 3.9 Hz, 3 H, SiMe₂). Satisfactory elemental analysis could not be obtained.

Crystal structure determinations for [NbCp{ η^3 -N(Ar)SiMe₂-H}Cl(PMe₃)] (**6**), [TaCp(NAr)(H)(SiMe₂Cl)(PMe₃)] (**8**) and [CpTa(NAr)(Cl)(PMe₃)₂]OTf (**13**), and preliminary determination of [NbCp{ η^3 -N(Ar')SiMe₂-H}Cl(PMe₃)] (**7**)

Crystal data collection and processing parameters are given in Table 7. The crystals of **6** and **7** were grown from pentane, crystals of **8** and **13** from ether. For all compounds the crystal was mounted in a film of perfluoropolyether oil on a glass fibre and transferred to the diffractometer (Stoë Stadi-4 for **6** and Siemens three-circle diffractometer with a CCD detector (SMART system) for **7**, **8** and **13**). For all structures the data were corrected for Lorentz and polarisation effects. The structures were solved by direct methods⁵¹ and refined by full-matrix least squares procedures.⁵² For compounds **6**, **8** and **13** non-hydrogen atoms were refined anisotropically. All hydrogen atoms except the hydrides (which were located from Fourier difference synthesis and positionally refined isotropically for **6** and **8**) were placed in calculated positions and refined in a “riding” model.

In the case of **7** all crystals analysed were of unsatisfactory quality with a typical reflection width of more than 2°. Nevertheless the data were collected and the structure solved as described. Although only an isotropic refinement could be carried out, this allowed us to establish with confidence the positions of the non-hydrogen atoms. Final *R* factor (all data) was 0.3081. Selected distances and angles and a view of the molecular structure of **7** are provided as ESI. †

CCDC reference numbers 133301, 133302 and 164933.

See <http://www.rsc.org/suppdata/dt/b1/b103362j/> for crystallographic data in CIF or other electronic format.

Computational details

Calculations on the model **16d** (see Table 4, footnote *b*) were carried out as described in our initial communication.²⁵ All other calculations were carried out with the Gaussian 98 program package⁵³ using density functional theory applying Becke’s 1988 non-local exchange functional⁵⁴ in conjunction with Perdew’s correlation functional,⁵⁵ commonly aliased as BP86. Three different models were employed to describe the structure, energies and electronic distribution of the niobium complexes **6** and **7** as described in the Computational studies section. The compound basis set used for the calculation in Model 2 consisted of the 6-31G(d) basis set for the nitrogen and the carbon atoms of the Cp ring, the 3-21G basis set for the phenyl group and the hydrogens of the Cp ring, as well as for the H-substituents at the P and Si atoms. The Hay–Wadt VDZ effective core potentials (ECP) and the corresponding VDZ basis sets⁵⁶ were used for the niobium atom, and the “Stuttgart” quasi-relativistic ECP⁵⁷ were used for the atoms Si, P and Cl in this model. In order to describe properly the position of the H atom, the 6-31G basis set augmented by the *p*-polarization function (6-31G(d,p) basis set) was used. The more complicated Model 3 employed the (full-electron) 6-31G(d) basis sets for the Si, N, P atoms, the 6-31G basis sets for the methyl substituents at the Si, and P and the carbon atoms comprising the Cp ring. The hydrogen atoms of the Cp ring as well as the atoms of the phenyl group were described in Model 3 with the 3-21G basis set. As in Model 2, the Hay–Wadt ECP⁵⁶ for the niobium atom, the “Stuttgart” ECP⁵⁷ for the chlorine atom, and the 6-31G basis set augmented with polarization *p*-function for the hydride were used. Full geometry optimizations for all of the molecular structures were performed. Natural bond orbital analyses were performed with the Gaussian NBO 3.1 program incorporated in the Gaussian 98 package. For this purpose, the Kohn–Sham orbitals resulting from the DFT calculations were employed.

Acknowledgements

This work was generously supported by the Royal Society (London) through a Joint Research Grant to P. M., D. A. L. and G. I. N. G. I. N. is also grateful to the Royal Society of Chemistry for a Grant for International Authors. S. K. I. and

A. G. R. thank the Russian Fund for Basic Research RFBR for financial support. J. A. K. H. thanks the EPSRC for a Senior Research Fellowship.

References

- (a) J. K. Hoyano, M. Elder and W. A. K. Graham, *J. Am. Chem. Soc.*, 1969, **96**, 4568; (b) for an overview of earlier ideas see W. A. K. Graham, *J. Organomet. Chem.*, 1986, **300**, 81 and references therein.
- M. Brookhart and M. L. H. Green, *J. Organomet. Chem.*, 1983, **250**, 395.
- (a) L. J. Procopio, P. J. Carroll and D. H. Berry, *J. Am. Chem. Soc.*, 1994, **116**, 177; (b) W. A. Herrmann, N. W. Huber and J. Behm, *Chem. Ber.*, 1992, **125**, 1405; (c) W. A. Herrmann, J. Eppinger, M. Spiegler, O. Runte and R. Anwender, *Organometallics*, 1997, **16**, 1813; (d) A. Ohff, P. Kosse, W. Baumann, A. Tillack, R. Kempe, H. Görls, V. V. Burlakov and U. Rosenthal, *J. Am. Chem. Soc.*, 1995, **117**, 10399; (e) U. Schubert, M. Schwartz and F. Möller, *Organometallics*, 1994, **13**, 1554; (f) J. Yin, J. Klozin, K. Abboud and W. M. Jones, *J. Am. Chem. Soc.*, 1995, **117**, 3298; (g) U. Schubert and H. Giges, *Organometallics*, 1995, **15**, 2373; (h) I. Nagl, W. Scherer, M. Tafipolsky and R. Anwender, *Eur. J. Inorg. Chem.*, 1999, 1405; (i) J. Eppinger, M. Spiegler, W. Hieringer, W. A. Herrmann and R. Anwender, *J. Am. Chem. Soc.*, 2000, **122**, 3080.
- G. J. Kubas, R. R. Ryan, B. I. Swanson, P. J. Vergamini and H. J. Wasserman, *J. Am. Chem. Soc.*, 1984, **106**, 451.
- (a) O. B. Gritsenko, A. A. Bagatur'yants and I. I. Moiseev, *Kinet. Katal.*, 1980, **21**, 632; (b) M. B. Kuzminskii, A. A. Bagatur'yants, G. M. Zhidomirov and V. B. Kazanskii, *Kinet. Katal.*, 1980, **22**, 151; (c) O. B. Gritsenko, A. A. Bagatur'yants, I. I. Moiseev and I. V. Kalechits, *Kinet. Katal.*, 1980, **22**, 354; (d) O. B. Gritsenko, V. A. Korsunov, A. A. Bagatur'yants, I. I. Moiseev and I. V. Kalechits, *Kinet. Katal.*, 1980, **22**, 1431; (e) A. A. Bagatur'yants, N. A. Anikin, G. M. Zhidomirov and V. B. Kazanskii, *Zh. Fiz. Khim.*, 1981, **55**, 2035.
- R. H. Crabtree, *Angew. Chem., Int. Ed. Engl.*, 1993, **32**, 789.
- U. Schubert, *Adv. Organomet. Chem.*, 1990, **30**, 151.
- (a) J. Kubas, *Acc. Chem. Res.*, 1988, **21**, 120; (b) R. H. Crabtree, *Acc. Chem. Res.*, 1990, **23**, 95; (c) D. H. Heinekey and W. J. Oldham, Jr., *Chem. Rev.*, 1993, **93**, 913; (d) P. J. Jessop and R. H. Morris, *Coord. Chem. Rev.*, 1992, **121**, 155.
- D. R. Evans, T. Drovetskaya, R. Bau, C. Reed and P. D. W. Boyd, *J. Am. Chem. Soc.*, 1997, **119**, 3633.
- F. Carré, E. Colomer, R. J. P. Corriu and A. Vioux, *Organometallics*, 1984, **3**, 1272.
- U. Schubert, E. Kunz, B. Harkers, J. Willnecker and J. Meyer, *J. Am. Chem. Soc.*, 1989, **111**, 2572.
- See for example: C. N. Muhoro, X. He and J. F. Hartwig, *J. Am. Chem. Soc.*, 1999, **121**, 5033.
- (a) R. Tomaszewski, I. Hyla-Kryspin, C. L. Mayne, A. M. Arif, R. Gleiter and R. D. Ernst, *J. Am. Chem. Soc.*, 1998, **120**, 2959; (b) W. T. Klooster, L. Brammer, C. J. Schaverien and P. H. M. Budzelaar, *J. Am. Chem. Soc.*, 1999, **121**, 1381.
- M. D. Butts, J. C. Bryan, X.-L. Luo and G. Kubas, *Inorg. Chem.*, 1997, **36**, 3341.
- (a) M. J. S. Dewar, *Bull. Soc. Chim. Fr.*, 1951, **18**, C79; (b) J. Chatt and L. A. Duncanson, *J. Chem. Soc.*, 1953, 2939.
- O. Eisenstein and Y. Jean, *J. Am. Chem. Soc.*, 1985, **107**, 1177.
- A. Haaland, W. Scherer, K. Ruud, S. McGrady, A. J. Downs and O. Swang, *J. Am. Chem. Soc.*, 1998, **120**, 3762.
- M.-F. Fan and Z. Lin, *Organometallics*, 1997, **16**, 494.
- (a) G. C. Pimentel, *J. Chem. Phys.*, 1951, **19**, 446; (b) R. J. Hach and R. E. Rundel, *J. Am. Chem. Soc.*, 1951, **73**, 4321; (c) J. I. Musher, *Angew. Chem., Int. Ed. Engl.*, 1969, **8**, 54.
- (a) G. I. Nikonov, L. G. Kuzmina, D. A. Lemenovskii and V. V. Kotov, *J. Am. Chem. Soc.*, 1995, **117**, 10133; (b) G. I. Nikonov, L. G. Kuzmina, D. A. Lemenovskii and V. V. Kotov, *J. Am. Chem. Soc.*, 1996, **118**, 6333 (corr.); (c) G. I. Nikonov, L. G. Kuzmina, S. F. Vyboishchikov, D. A. Lemenovskii and J. A. K. Howard, *Chem. Eur. J.*, 1999, **5**, 2497; (d) S. B. Duckett, L. G. Kuzmina and G. I. Nikonov, *Inorg. Chem. Commun.*, 2000, **3**, 126; (e) V. I. Bakmutov, J. A. K. Howard, D. A. Keen, L. G. Kuzmina, M. A. Leech, G. I. Nikonov, E. V. Vorontsov and C. C. Wilson, *J. Chem. Soc., Dalton Trans.*, 2000, 1631.
- No IHI was detected in the bis(tin) complex $Cp_2Nb(SnMe_2Cl)_2H$ analogous to D: G. I. Nikonov, L. G. Kuzmina and J. Lorberth, *Eur. J. Inorg. Chem.*, 1999, 825.
- For calculations at the MP2 level see M.-F. Fan and Z. Lin, *Organometallics*, 1998, **17**, 1092.
- T. I. Gountchev and T. D. Tilley, *J. Am. Chem. Soc.*, 1997, **119**, 12831.
- (a) D. S. Williams, M. H. Schofield and R. R. Schrock, *Organometallics*, 1993, **12**, 4560; (b) D. N. Williams, J. P. Mitchell, A. D. Pool, U. Siemeling, W. Clegg, D. C. R. Hockless, P. A. O'Neil and V. C. Gibson, *J. Chem. Soc., Dalton Trans.*, 1992, 739; (c) J. Sundermeyer and D. Runge, *Angew. Chem., Int. Ed. Engl.*, 1994, **33**, 1255.
- G. I. Nikonov, P. Mountford, J. C. Green, P. A. Cooke, M. A. Leech, A. J. Blake, J. A. K. Howard and D. A. Lemenovskii, *Eur. J. Inorg. Chem.*, 2000, 1917.
- U. Siemeling and V. C. Gibson, *J. Organomet. Chem.*, 1992, **426**, C25.
- M. C. W. Chan, J. M. Cole, V. C. Gibson, J. A. K. Howard, C. Lehmann, A. D. Poole and U. Siemeling, *J. Chem. Soc., Dalton Trans.*, 1998, 103.
- S. Schmidt and J. Sundermeyer, *J. Organomet. Chem.*, 1994, **472**, 127.
- (a) H. G. Alt and H. E. Engelhardt, *Z. Naturforsch., Teil B*, 1989, **44**, 367; (b) A. Zaki, L. G. Hubert-Pfalzgraf and L. Toupet, *Acta Crystallogr., Sect. C*, 1991, **47**, 533.
- (a) M. D. Curtis, L. G. Bell and N. M. Buter, *Organometallics*, 1985, **4**, 701; (b) A. Antiñolo, F. Carrillo, M. Fajardo, A. Otero, M. Lanfranchi and M. A. Pellinghelli, *Organometallics*, 1995, **14**, 1518; (c) G. I. Nikonov, L. G. Kuzmina and J. A. K. Howard, *Organometallics*, 1997, **16**, 3723 and references therein.
- (a) U. Burckhardt and T. D. Tilley, *J. Am. Chem. Soc.*, 1999, **121**, 6328; (b) U. Burckhardt, G. L. Casty, T. D. Tilley, T. K. Woo and U. Rothlisberger, *Organometallics*, 2000, **19**, 3830.
- (a) G. I. Nikonov, D. A. Lemenovskii and J. Lorberth, *Organometallics*, 1994, **13**, 3127; (b) G. I. Nikonov, K. Harms, J. Lorberth and D. A. Lemenovskii, *Inorg. Chem.*, 1995, **34**, 2461; (c) G. I. Nikonov, L. G. Kuzmina, Yu. K. Grishin, D. A. Lemenovskii and N. B. Kazennova, *J. Organomet. Chem.*, 1997, **547**, 183; (d) G. I. Nikonov, A. J. Blake, J. Lorberth, D. A. Lemenovskii and S. Wocadlo, *J. Organomet. Chem.*, 1997, **547**, 235; (f) G. I. Nikonov, E. V. Avtomonov and W. Massa, *Chem. Ber.*, 1997, **130**, 1629.
- V. I. Bakmutov, E. V. Vorontsov, G. I. Nikonov and D. A. Lemenovskii, *Inorg. Chem.*, 1998, **37**, 279.
- (a) L. J. Procopio, P. J. Carroll and D. H. Berry, *J. Am. Chem. Soc.*, 1991, **113**, 1870; (b) L. J. Procopio, P. J. Carroll and D. H. Berry, *Polyhedron*, 1995, **14**, 45.
- J. Arnold, T. D. Tilley, A. L. Rheingold and S. J. Geib, *Organometallics*, 1987, **6**, 473.
- (a) J. M. Mayer, C. J. Curtis and J. E. Bercaw, *J. Am. Chem. Soc.*, 1983, **105**, 2651; (b) D. M. Antonelli, W. P. Schaefer, G. Parkin and J. E. Bercaw, *J. Organomet. Chem.*, 1991, **462**, 213; (c) G. Parkin, A. van Asset, D. J. Leahy, L. Whinnery, N. G. Nua, R. W. Quan, L. M. Henling, W. P. Schaefer, B. D. Santarsiero and J. E. Bercaw, *Inorg. Chem.*, 1992, **31**, 82; (d) S. R. Huber, T. C. Baldwin and D. E. Wigley, *Organometallics*, 1993, **12**, 91; (e) A. N. Chernega, M. L. H. Green and A. G. Suarez, *J. Chem. Soc., Dalton Trans.*, 1993, 3031; (f) M. L. H. Green and P. C. Konidaris, *J. Chem. Soc., Dalton Trans.*, 1994, 2975.
- (a) K. E. Lee, A. M. Arif and J. A. Gladysz, *Chem. Ber.*, 1991, **124**, 309; (b) B. R. Jagirdar, R. Palmer, K. J. Klabunde and L. Radonovich, *Inorg. Chem.*, 1995, **34**, 278; (c) M. K. Hays and R. Eisenberg, *Inorg. Chem.*, 1991, **30**, 2623; (d) T. S. Koloski, D. C. Pestana, P. J. Carroll and D. H. Berry, *Organometallics*, 1994, **13**, 489.
- The United Kingdom Chemical Database Service; D. A. Fletcher, R. F. McMeeking and D. Parkin, *J. Chem. Inf. Comput. Sci.*, 1996, **36**, 746.
- (a) G. I. Nikonov, P. Mountford, L. G. Kuzmina, J. A. K. Howard, D. A. Lemenovskii and D. M. Roitershtein, *J. Organomet. Chem.*, 2001, **628**, 25; (b) J. Sundermeyer, U. Radius and C. Burschka, *Chem. Ber.*, 1992, **125**, 2379; (c) A. K. Kohler, H. W. Roesky, A. Herzog, H. Gornitzka, A. Steiner and I. Uson, *Inorg. Chem.*, 1996, **35**, 1773; (d) P. Gomez Sal, I. Jimenez, A. Martin, T. Pedraz, P. Royo, A. Selles and A. Vazquez de Miguel, *Inorg. Chem. Acta*, 1998, **273**, 270.
- U. Radius and J. Sundermeyer, *Chem. Ber.*, 1992, **125**, 2183.
- D. M. Antonelli, M. L. H. Green and P. Mountford, *J. Organomet. Chem.*, 1992, **438**, C4.
- D. J. Arney, M. A. Bruck, S. R. Huber and D. E. Wigley, *Inorg. Chem.*, 1992, **31**, 3749.
- J. K. Cockcroft, V. C. Gibson, J. A. K. Howard, A. D. Pool, U. Siemeling and C. Wilson, *J. Chem. Soc., Chem. Commun.*, 1992, 1668.
- M. V. Galakhov, M. Gomez, G. Jimenez, M. A. Pellinghelli, P. Royo and A. Tiripicchio, *Organometallics*, 1994, **13**, 1564.
- For a recent review (a) F. Maseras, A. Lledós, E. Clot and O. Eisenstein, *Chem. Rev.*, 2000, **100**, 601; some examples: (b) F. Maseras and A. Lledós, *Organometallics*, 1996, **15**, 1218; (c) M.-F. Fan, G. Jia and Z. Lin, *J. Am. Chem. Soc.*, 1996, **118**, 9915;

- (d) F. Maseras, A. Lledós, M. Costas and J. M. Poblet, *Organometallics*, 1996, **15**, 2947; (e) R. Gelabert, M. Moreno, J. M. Lluch and A. Lledós, *J. Am. Chem. Soc.*, 1997, **119**, 9840; (f) M.-F. Fan and Z. Lin, *Organometallics*, 1997, **16**, 494; (g) H. Jacobsen and H. Berke, *Chem. Eur. J.*, 1997, **3**, 881; (h) J. Tomas, A. Lledós and Y. Jean, *Organometallics*, 1998, **17**, 190.
- 46 P. Kubacek, R. Hoffmann and Z. Havlas, *Organometallics*, 1982, **1**, 180.
- 47 Z. Lin and M. B. Hall, *Organometallics*, 1993, **12**, 19.
- 48 P. D. Lyne and D. M. P. Mingos, *J. Organomet. Chem.*, 1994, **478**, 141; P. D. Lyne and D. M. P. Mingos, *J. Chem. Soc., Dalton Trans.*, 1995, 1635; E. M. Shustorovich, M. A. Porai-Koshits and Y. A. Buslaev, *Coord. Chem. Rev.*, 1975, **17**, 1; N. Kaltsoyannis and P. Mountford, *J. Chem. Soc., Dalton Trans.*, 1999, 781; B. J. Coe and S. J. Glenwright, *Coord. Chem. Rev.*, 2000, **203**, 5; J. K. Burdett and T. A. Albright, *Inorg. Chem.*, 1979, **18**, 2112.
- 49 W. Wolfsberger and H. Schmidbaur, *Synth. React. Inorg. Met.-Org. Chem.*, 1974, **4**, 149.
- 50 A. M. Cardoso, R. J. H. Clark and S. Moorhouse, *J. Chem. Soc., Dalton Trans.*, 1980, 1156.
- 51 (a) G. M. Sheldrick, SHELXS-86, Program for Crystal Structure Solution, *Acta Crystallogr., Sect. A*, 1990, **146**, 467; (b) A. Altomare, G. Casciarano, G. Giacovazzo, A. Guagliardi, M. C. Burla, G. Polidori and M. Camalli, *J. Appl. Crystallogr.*, 1994, **27**, 435.
- 52 (a) G. M. Sheldrick, SHELXTL-96, Program for Crystal Structure Refinement, Universität Göttingen, 1996; (b) D. J. Watkin, C. K. Prout, J. R. Carruthers and P. W. Betteridge, CRYSTALS Issue 10, Chemical Crystallography Laboratory, University of Oxford, 1996.
- 53 Gaussian 98, Revision A.3, M. J. Frisch, G. W. Trucks, H. B. Schlegel, G. E. Scuseria, M. A. Robb, J. R. Cheeseman, V. G. Zakrzewski, J. A. Montgomery, Jr., R. E. Stratmann, J. C. Burant, S. Dapprich, J. M. Millam, A. D. Daniels, K. N. Kudin, M. C. Strain, O. Farkas, J. Tomasi, V. Barone, M. Cossi, R. Cammi, B. Mennucci, C. Pomelli, C. Adamo, S. Clifford, J. Ochterski, G. A. Petersson, P. Y. Ayala, Q. Cui, K. Morokuma, D. K. Malick, A. D. Rabuck, K. Raghavachari, J. B. Foresman, J. Cioslowski, J. V. Ortiz, B. B. Stefanov, G. Liu, A. Liashenko, P. Piskorz, I. Komaromi, R. Gomperts, R. L. Martin, D. J. Fox, T. Keith, M. A. Al-Laham, C. Y. Peng, A. Nanayakkara, C. Gonzalez, M. Challacombe, P. M. W. Gill, B. Johnson, W. Chen, M. W. Wong, J. L. Andres, C. Gonzalez, M. Head-Gordon, E. S. Replogle and J. A. Pople, Gaussian, Inc., Pittsburgh, PA, 1998.
- 54 A. D. Becke, *Phys. Rev. A*, 1988, **38**, 3098.
- 55 B. P. Perdew, *Phys. Rev. B*, 1986, **33**, 8822.
- 56 P. J. Hay and W. R. Wadt, *J. Chem. Phys.*, 1985, **82**, 299.
- 57 A. Bergner, M. Dolg, W. Kuechle, H. Stoll and H. Preuss, *Mol. Phys.*, 1993, **80**, 1431.